fractal and fractional

Article

Spectral Galerkin Methods for Riesz Space-Fractional Convection–Diffusion Equations

Xinxia Zhang, Jihan Wang, Zhongshu Wu, Zheyi Tang and Xiaoyan Zeng *

Department of Mathematics, Shanghai University, Shanghai 200444, China
* Correspondence: cherryzxy@shu.edu.cn

Abstract: This paper applies the spectral Galerkin method to numerically solve Riesz space-fractional convection–diffusion equations. Firstly, spectral Galerkin algorithms were developed for one-dimensional Riesz space-fractional convection–diffusion equations. The equations were solved by discretizing in space using the Galerkin–Legendre spectral approaches and in time using the Crank–Nicolson Leap-Frog (CNLF) scheme. In addition, the stability and convergence of semi-discrete and fully discrete schemes were analyzed. Secondly, we established a fully discrete form for the two-dimensional case with an additional complementary term on the left and then obtained the stability and convergence results for it. Finally, numerical simulations were performed, and the results demonstrate the effectiveness of our numerical methods.

Keywords: Riesz fractional derivatives; fractional convection–diffusion equation; spectral Galerkin method

1. Introduction

Fractional calculus theory is a generalization of traditional calculus theory that extends the order of derivatives from integers to real numbers. Compared with conventional differential equations, fractional differential equations can better simulate physical processes in nature due to the non-locality of the fractional derivatives. Fractional differential equations have been extensively researched in various fields, including mechanics, statistics, physics, biology, economics, and finance [1–8].

Fractional differential equations are typically challenging to solve due to the non-locality of fractional differential operators. Some fractional differential equations can be solved using the Fourier transform, Laplace transform, Mellin transform, or Green function [9–12]. However, these solutions typically involve complex and specialized functions that are challenging to calculate, such as Mittag-Leffler functions, Wright functions, hypergeometric functions, etc. As a matter of fact, for the vast majority of fractional differential equations, the analytical solution cannot be found. Therefore, it is crucial to develop efficient and stable numerical algorithms for them. Numerical algorithms for fractional differential equations mainly include the finite difference method, finite element method, and spectral method. The spectral method differs from the first two methods in that it utilizes trigonometric functions or orthogonal polynomials as basis functions for numerical approximation, which contributes to its high convergence. The higher the regularity of the true solution, the smaller the error of the numerical solution. If the exact solution of the equation is infinitely smooth, then the spectral method can achieve convergence accuracy of "infinite order". In 1994, Blinova proposed the concept of spectral methods. In the 1980s, Gottlieb et al. extended the spectral method to solve a wide range of problems and conducted systematic theoretical analysis. In the 1990s, spectral methods were widely used in fluid mechanics calculations [13].

The fractional convection–diffusion equation is a significant application of fractional partial differential equations and is extensively utilized in science and engineering. Fractional differential equations can be directly used to describe anomalous diffusion phenomena [14]. The non-Gaussian diffusion process can be described using fractional derivatives,

check for updates

Citation: Zhang, X.; Wang, J.; Wu, Z.; Tang, Z.; Zeng, X. Spectral Galerkin Methods for Riesz Space-Fractional Convection–Diffusion Equations. *Fractal Fract.* **2024**, *8*, 431. https://doi.org/10.3390/fractalfract8070431

Academic Editor: Bruce Henry

Received: 11 June 2024
Revised: 11 July 2024
Accepted: 19 July 2024
Published: 22 July 2024

such as the Caputo fractional derivative, the Riemann–Liouville fractional derivative, or the Riesz fractional derivative [15,16]. In general, the Caputo derivative is often used in the temporal domain to represent the historical dependence in the time direction. The Riemann–Liouville derivatives or Riesz fractional derivatives are often used in the spatial direction to characterize long-distance interactions [17–20].

The Riesz fractional derivatives on a finite domain $[a, b]$ are defined as follows:

$$\frac{\partial^\gamma u}{\partial |x|^\gamma} = c_\gamma \left({}_aD_x^\gamma u + {}_xD_b^\gamma u \right), \quad 0 < \gamma < 2, \gamma \neq 1,$$

where $c_\gamma = -1/(2\cos(\gamma\pi/2))$, and for $n-1 \leq \gamma < n, n \in \mathbb{N}$, the operators ${}_aD_x^\gamma$, ${}_xD_b^\gamma$ are

$$\begin{aligned} {}_aD_x^\gamma u &= \frac{1}{\Gamma(n-\gamma)} \frac{\partial^n}{\partial x^n} \int_a^x \frac{u(s)}{(x-s)^{\gamma-n+1}} ds, \\ {}_xD_b^\gamma u &= \frac{(-1)^n}{\Gamma(n-\gamma)} \frac{\partial^n}{\partial x^n} \int_x^b \frac{u(s)}{(s-x)^{\gamma-n+1}} ds. \end{aligned}$$

From the above definition, we can see that the Riesz fractional derivative includes both left and right Riemann–Liouville fractional derivatives. This indicates that a state depends on information not only on the left side but also on the right side. For more details, please refer to [1].

There have been numerous studies on the numerical solution of fractional-order (convection–) diffusion equations: Sun [21] used the $L1$ formula to approximate the time derivative and presented a difference scheme for the Caputo time-fractional diffusion-wave equation. Liu [22] proposed a random walk model to approximate the Lévy–Feller advection–dispersion process and provided an explicit finite difference approximation of the equation. Shen [23] used the shifted Grünward–Letnikov formula to approximate the spatial-fractional derivative, and the $L1$ formula to approximate the temporal fractional derivative. Shen provided explicit and implicit differences for the space–time Riesz-Caputo fractional advection–diffusion equation. Zhou [24] proposed a compact finite difference scheme for the space-fractional diffusion equation. Wang [25] proposed a fast characteristic finite difference method for solving space-fractional advection–diffusion equations. Huang [26] provided the finite element solution for the fractional advection–dispersion equation. Lai [27] obtained a space–time finite element method for linear Riesz space-fractional partial differential equations. Tang [28] proposed the discontinuous Galerkin method combined with the Runge–Kutta method for solving the spatial-fractional diffusion equation. Bhrawy [29] utilized the shifted Jacobi polynomial as the basis function to construct a matrix of fractional differential operators and proposed a Jacobi spectral collocation method for nonlinear fractional sub-diffusion equations. Afterward, Bhrawy [30] introduced the spectral tau method for the two-sided space–time Caputo fractional diffusion-wave equation. This method utilized the shifted Legendre polynomial as the basis function to construct a fractional differential matrix. Saadatmandi [31] utilized the Sinc–Legendre configuration method to provide a numerical approximation of a series of variable-coefficient fractional convection–diffusion equations.

For the convection–diffusion equation with Riesz fractional derivatives, Shen [32] utilized the Laplace transform and Fourier transform to derive the exact solution of the Riesz space-fractional convection–diffusion equation. Additionally, the finite difference formulation is provided using the Grünward–Letnikov formula. Yang [33] established the relationship between the Laplace operator and the Riesz fractional differential operator and used the eigenequation $-\Delta\phi = \lambda\phi$ to derive the analytical solution of the Riesz spatial diffusion equation. Moreover, the $L1$ / $L2$ approximation method, the displacement Grünward formula method, and the matrix transformation method (MTM) were employed to approximate the fractional derivative. Zhang [34] proposed the Galerkin finite element approximation of the Riesz space-fractional convection–diffusion equation. Celik [35] presented the Crank–Nicolson method for solving the Riesz space-fractional diffusion equation. Zeng [36] proposed the Crank–Nicolson Alternating Direction Implicit (ADI) method for solving the Riesz nonlinear reaction–diffusion equation. Anley [37] discussed the finite difference method for a two-sided two-dimensional space-fractional convection–diffusion problem with a source term. Basha [38] derived a linearized Crank–Nicolson scheme for the two-dimensional nonlinear Riesz space-fractional convection–diffusion equation.

Recently, some researchers have been exploring numerical solutions for distribution-order differential equations. For example, Li [39,40] considered the finite volume method for the Riesz spatial distribution-order diffusion equation and the convection–diffusion equation, respectively. Ye [41] presented an implicit difference scheme for time distributed-order and Riesz space-fractional diffusion equations. Zhang [42] proposed the Crank–Nicolson ADI Galerkin–Legendre spectral method for solving the two-dimensional Riesz space distributed-order advection–diffusion equation. Hu [43] introduced a new definition of the spatial derivative and provided the implicit difference scheme for the space-fractional advection–dispersion equation.

In this paper, we consider the below Riesz space-fractional convection–diffusion equations [37,44]:

$$\begin{aligned} &\frac{\partial u(\boldsymbol{x},t)}{\partial t} = \sum_{i=1}^{d} K_i \frac{\partial^{\gamma_i^{(1)}} u(\boldsymbol{x},t)}{\partial |x_i|^{\gamma_i^{(1)}}} + \sum_{i=1}^{d} K_{d+i} \frac{\partial^{\gamma_i^{(2)}} u(\boldsymbol{x},t)}{\partial |x_i|^{\gamma_i^{(2)}}} + f(\boldsymbol{x},t),\ (\boldsymbol{x},t) \in \Omega_d \times I, \\ &u(\boldsymbol{x},0) = u_0(\boldsymbol{x}), \boldsymbol{x} \in \Omega_d, \\ &u(\boldsymbol{x},t) = 0, (\boldsymbol{x},t) \in \partial\Omega_d \times I, \end{aligned} \tag{1}$$

where $0 < \gamma_i^{(1)} < 1$, $1 < \gamma_i^{(2)} < 2$, $I = (0,T]$ is the time interval, $\Omega_d = (a_1,b_1) \times \cdots \times (a_d,b_d)$ is the d-dimensional spatial domain, $u(\boldsymbol{x},t)$ denotes the solute concentration, positive numbers of $K_i, i = 1,\cdots,d$ denote the fluid velocities in the x_i direction, positive numbers of $K_{d+i}, i = 1,\cdots,d$ denote the diffusion coefficients, and $f(\boldsymbol{x},t)$ is the source function.

We aim to apply the spectral Galerkin method to the above Riesz space-fractional convection–diffusion equations when $d = 1$ and $d = 2$ and derive a fast and efficient scheme for those equations. This paper is structured as follows. In Section 2, preliminaries for fractional derivatives are introduced. In Sections 3 and 4, the spectral Galerkin methods for solving one-dimensional and two-dimensional space-fractional convection–diffusion equations are presented, together with the analysis of the stability and convergence, respectively. Several numerical examples are provided in Section 5, and the results of these examples can validate the effectiveness of the proposed algorithms. This paper is summarized in Section 6.

2. Preliminaries

In this section, we will introduce the necessary notations and details in fractional calculus that are used throughout this paper.

Lemma 1. *If* $n-1 < \alpha < n,\ \hat{x} \in [-1,1]$, *then*

$$\begin{aligned} {}_{-1}D_{\hat{x}}^{\alpha}\Big((1+\hat{x})^{\delta+\alpha} J_n^{\gamma-\alpha,\delta+\alpha}(\hat{x})\Big) &= \frac{\Gamma(n+\delta+\alpha+1)}{\Gamma(n+\delta+1)}(1+x)^{\delta} J_n^{\gamma,\delta}(\hat{x}), \\ {}_{\hat{x}}D_{1}^{\alpha}\Big((1-\hat{x})^{\gamma+\alpha} J_n^{\gamma+\alpha,\delta-\alpha}(\hat{x})\Big) &= \frac{\Gamma(n+\gamma+\alpha+1)}{\Gamma(n+\gamma+1)}(1-x)^{\gamma} J_n^{\gamma,\delta}(\hat{x}), \end{aligned}$$

where $J_n^{\alpha,\beta}(\hat{x})(\alpha,\beta > -1)$ *is the Jacobi polynomial [45].*

According to Lemma 1, the chain rule, and $L_n(\hat{x}) = J_n^{0,0}(\hat{x})$, we have the following lemma.

Lemma 2. *If $n-1<\alpha<n$, $\hat{x}\in[-1,1]$, $x=(b-a)\hat{x}/2+(b+a)/2\in[a,b]$, then*

$$\begin{aligned}
{}_aD_x^{\alpha}L_n(\hat{x}) &= \frac{1}{\Gamma(n-\alpha)}\frac{d^n}{dx^n}\int_a^x (x-s)^{n-\alpha-1}L_n(\hat{x})ds \\
&= (\frac{b-a}{2})^{-\alpha}\frac{\Gamma(n+1)}{\Gamma(n-\alpha+1)}(1+\hat{x})^{-\alpha}J_n^{\alpha,-\alpha}(\hat{x}), \hat{x}\in[-1,1], \\
{}_xD_b^{\alpha}L_n(\hat{x}) &= \frac{(-1)^n}{\Gamma(n-\alpha)}\frac{d^n}{dx^n}\int_x^b (s-x)^{n-\alpha-1}L_n(\hat{x})ds \\
&= (\frac{b-a}{2})^{-\alpha}\frac{\Gamma(n+1)}{\Gamma(n-\alpha+1)}(1-\hat{x})^{-\alpha}J_n^{-\alpha,\alpha}(\hat{x}), \hat{x}\in[-1,1],
\end{aligned}$$

where $L_n(\hat{x})$ is the Legendre polynomial [45], and $J_n^{\alpha,\beta}(\hat{x})(\alpha,\beta>-1)$ is the Jacobi polynomial.

Let d denote the dimensionality of the space. We choose $\Omega_d=(a_1,b_1)\times\cdots\times(a_d,b_d)\subset\mathbb{R}^d$ to be the space domain with $d=1$ or $d=2$ in this paper. Let $\mathcal{L}^2(\Omega_d)$ denote the $\mathcal{L}^2$-space on Ω_d, with the corresponding inner product being $(\cdot,\cdot)$ and the $\mathcal{L}^2$-norm being $\|\cdot\|_{\mathcal{L}^2(\Omega_d)}$. $C_0^{\infty}(\Omega_d)$ denotes the space consisting of all infinitely many successive differentiable functions on Ω_d with compact support. In the following, we present several function spaces.

Definition 1. *Define the seminorm*

$$|u|_{J_L^{\mu}(\Omega_d)} = \left(\sum_{i=1}^{d}\|{}_{a_i}D_{x_i}^{\mu}u(\boldsymbol{x})\|^2_{\mathcal{L}^2(\Omega_d)}\right)^{1/2},$$

and the norm

$$\|u\|_{J_L^{\mu}(\Omega_d)} = \left(\|u\|^2_{\mathcal{L}^2(\Omega_d)}+|u|^2_{J_L^{\mu}(\Omega_d)}\right)^{1/2},$$

for $\mu>0$. Here, $J_L^{\mu}(\Omega_d)$ ($J_{L,0}^{\mu}(\Omega_d)$) denotes the closure of $C^{\infty}(\Omega_d)$ ($C_0^{\infty}(\Omega_d)$) with respect to $\|\cdot\|_{J_L^{\mu}(\Omega_d)}$.

Definition 2. *Define the seminorm*

$$|u|_{J_R^{\mu}(\Omega_d)} = \left(\sum_{i=1}^{d}\|{}_{x_i}D_{b_i}^{\mu}u(\boldsymbol{x})\|^2_{\mathcal{L}^2(\Omega_d)}\right)^{1/2},$$

and the norm

$$\|u\|_{J_R^{\mu}(\Omega_d)} = \left(\|u\|^2_{\mathcal{L}^2(\Omega_d)}+|u|^2_{J_R^{\mu}(\Omega_d)}\right)^{1/2},$$

for $\mu>0$. Here, $J_R^{\mu}(\Omega_d)$ ($J_{R,0}^{\mu}(\Omega_d)$) denotes the closure of $C^{\infty}(\Omega_d)$ ($C_0^{\infty}(\Omega_d)$) with respect to $\|\cdot\|_{J_R^{\mu}(\Omega_d)}$.

Definition 3. *Define the seminorm*

$$|u|_{J_S^{\mu}(\Omega_d)} = \left(\sum_{i=1}^{d}|({}_{a_i}D_{x_i}^{\mu}u(\boldsymbol{x}),{}_{x_i}D_{b_i}^{\mu}u(\boldsymbol{x}))|\right)^{1/2}$$

and the norm

$$\|u\|_{J_S^{\mu}(\Omega_d)} = \left(\|u\|^2_{\mathcal{L}^2(\Omega_d)}+|u|_{J_S^{\mu}(\Omega_d)}\right)^{1/2},$$

for $\mu>0$. Here, $J_S^{\mu}(\Omega_d)$ ($J_{S,0}^{\mu}(\Omega_d)$) denotes the closure of $C^{\infty}(\Omega_d)$ ($C_0^{\infty}(\Omega_d)$) with respect to $\|\cdot\|_{J_S^{\mu}(\Omega_d)}$.

Definition 4 ([46]). *Define the seminorm*

$$|u|_{H^\mu(\Omega_d)} = \left\| |\omega|^\mu F(u)(\omega) \right\|_{\mathcal{L}^2(\mathbb{R}^d)}$$

and the norm

$$\|u\|_{H^\mu(\Omega_d)} = \left(\|u\|^2_{\mathcal{L}^2(\Omega_d)} + |u|_{H^\mu(\Omega_d)} \right)^{1/2},$$

for $\mu > 0$, where $F(u)(\omega)$ is the Fourier transform of the function $u(\boldsymbol{x})$. $H_0^\mu(\Omega_d)$ denotes the closure of C_0^∞ with respect to $\|\cdot\|_{H^\mu(\Omega_d)}$.

Lemma 3 ([42]). *Let $\mu > 0$ and $\Omega = (a, b)$, $\forall u \in H_0^\mu(\Omega)$, $v \in H_0^{\mu/2}(\Omega)$. We have*

$$\left({}_aD_x^\mu u, v \right) = \left({}_aD_x^{\mu/2} u, {}_xD_b^{\mu/2} v \right), \left({}_xD_b^\mu u, v \right) = \left({}_xD_b^{\mu/2} u, {}_aD_x^{\mu/2} v \right).$$

Lemma 4. *Let $\mu > 0$, $\mu \neq n - 1/2$, $n \in \mathbb{N}$. The spaces $J_{L,0}^\mu(\Omega_d)$, $J_{R,0}^\mu(\Omega_d)$, and $J_{S,0}^\mu(\Omega_d)$ are equivalent to $H_0^\mu(\Omega_d)$ and have equivalent norms and seminorms.*

Lemma 5 ([36]). *Let $\mu > 0$ and $\Omega = (a, b)$ for $u \in J_{L,0}^\mu(\Omega) \bigcap J_{R,0}^\mu(\Omega)$; then,*

$$\left({}_aD_x^\mu u, {}_xD_b^\mu u \right) = \cos(\mu\pi) \|{}_{-\infty}D_x^\mu \hat{u}\|^2_{\mathcal{L}^2(\mathbb{R})} = \cos(\mu\pi) \|{}_xD_\infty^\mu \hat{u}\|^2_{\mathcal{L}^2(\mathbb{R})},$$

where $\hat{u}$ is the extension of u by zero outside Ω. If $\mu \neq n - 1/2$, $n \in \mathbb{N}$ and $u \in J_{L,0}^\mu(\Omega)$, then there exists a constant C independent of u such that

$$|\hat{u}|_{J_L^\mu(\mathbb{R})} \leq C|u|_{J_L^\mu(\Omega)}.$$

Note that there are also results similar to the above lemma for the two-dimensional case. Please refer to [36].

Lemma 6 ([36]). *Let $\mu > 0$. If $u \in H_0^\mu(\Omega_d)$, then there exists a constant $C_1 < 1$ such that*

$$C_1 \|u\|_{H_0^\mu(\Omega_d)} \leq |u|_{H_0^\mu(\Omega_d)} \leq \|u\|_{H_0^\mu(\Omega_d)}.$$

3. Spectral Galerkin Methods for One-Dimensional Riesz Space-Fractional Convection–Diffusion Equation

In this section, we focus on the following one-dimensional Riesz space-fractional convection–diffusion equation for $0 < \alpha_1 < 1, 1 < \alpha_2 < 2$:

$$\begin{aligned} \frac{\partial u(x,t)}{\partial t} &= K_1 \frac{\partial^{\alpha_1} u(x,t)}{\partial |x|^{\alpha_1}} + K_2 \frac{\partial^{\alpha_2} u(x,t)}{\partial |x|^{\alpha_2}} + f(x,t), a < x < b, 0 < t \leq T, \\ u(x,0) &= u_0(x), \quad a < x < b, \\ u(a,t) &= u(b,t) = 0, \quad 0 < t \leq T, \end{aligned} \tag{2}$$

where $u(x,t)$ is the solute concentration, K_1 is the diffusion coefficient, K_2 is the fluid velocity, and $f(x,t)$ is the source function.

Regarding problem (2), we can first obtain the semi-discrete form in time and then discretize it in space.

In the temporal direction, we utilize the CNLF scheme for discretization. The time step is taken to be $\tau = T/n_T$, $t_n = n\tau (n = 0, 1, \cdots, n_T)$. Equation (2) is approximated at time t_n as follows:

$$\frac{u(x,t_{n+1}) - u(x,t_{n-1})}{2\tau} = K_1 \frac{\partial^{\alpha_1}}{\partial |x|^{\alpha_1}} \frac{u(x,t_{n+1}) + u(x,t_{n-1})}{2} + K_2 \frac{\partial^{\alpha_2}}{\partial |x|^{\alpha_2}} \frac{u(x,t_{n+1}) + u(x,t_{n-1})}{2} + f(x,t_n) + O(\tau^2), \tag{3}$$

where the derivative with respect to time on the left is approximated by using the Leap-Frog scheme, the center average is used for u on the right, and the source function is taken at the value of t_n. Let

$$\delta_{\hat{t}} u^n = \frac{u^{n+1} - u^{n-1}}{2\tau}, u^{\bar{n}} = \frac{u^{n+1} + u^{n-1}}{2}; f^n = f(x,t_n).$$

Then, the semi-discrete form of Equation (2) at time t_n is

$$\delta_{\hat{t}} u^n = K_1 \frac{\partial^{\alpha_1}}{\partial |x|^{\alpha_1}} u^{\bar{n}} + K_2 \frac{\partial^{\alpha_2}}{\partial |x|^{\alpha_2}} u^{\bar{n}} + f^n. \tag{4}$$

$$\phi_k(x) = L_k(\hat{x}) - L_{k+2}(\hat{x}),\ \hat{x} \in [-1,1], \tag{5}$$

where $x = (b-a)\hat{x}/2 + (b+a)/2 \in [a,b]$, and $L_k(\hat{x})$ is the Legendre polynomial of degree k, satisfying the following triple-recurrence formula:

$$L_{k+1}(\hat{x}) = \frac{2k+1}{k+1} \hat{x} L_k(\hat{x}) - \frac{k}{k+1}(\hat{x}), \hat{x} \in [-1,1],$$
$$L_0(\hat{x}) = 1.$$

Define V_N as the function space spanned by $\{\phi_k(x)\}$, i.e.,

$$V_N = \text{span}\{\phi_0(x), \phi_1(x), \phi_2(x), \cdots, \phi_{N-2}(x)\},$$

the numerical solution of (2) is then obtained by finding $u_N^n \in V_N$ such that $\forall v \in V_N$ satisfies

$$\begin{cases} (\delta_{\hat{t}} u_N^n, v) = K_1 (\frac{\partial^{\alpha_1}}{\partial |x|^{\alpha_1}} u_N^{\bar{n}}, v) + K_2 (\frac{\partial^{\alpha_2}}{\partial |x|^{\alpha_2}} u_N^{\bar{n}}, v) + (f^n, v), \\ u_N^0 = \Pi_N^{1,0} u_0, \end{cases} \tag{6}$$

where $\Pi_N^{1,0}$ is the projection operator, which is defined as follows:

$$\left(\Pi_N^{1,0} u - u, v\right) + \left(\partial_x (\Pi_N^{1,0} u - u), \partial_x v\right) = 0, \quad \forall v \in V_N.$$

Because u_N^n is in the space of V_N, u_N^n can be written as

$$u_N^n(x) = \sum_{j=0}^{N-2} \hat{u}_j^n \phi_j(x). \tag{7}$$

Substituting u_N^n and v in (6) by the right-hand side of (7), we obtain the following system of linear equations:

$$(M - \tau S) U^{n+1} = (M + \tau S) U^{n-1} + 2\tau F^n, \tag{8}$$

where

$$
\begin{aligned}
(M)_{ij} &= (\phi_j, \phi_i),\\
(S)_{ij} &= K_1 c_{\alpha_1}(S^{\alpha_1} + (S^{\alpha_1})^T) + K_2 c_{\alpha_2}(S^{\alpha_2} + (S^{\alpha_2})^T),\\
(S^{\alpha_k})_{ij} &= \left({}_aD_x^{\alpha_k/2}\phi_j, {}_xD_b^{\alpha_k/2}\phi_i\right),\\
U^{n+1} &= (\hat{u}_0^{n+1}, \hat{u}_1^{n+1}, \hat{u}_2^{n+1}, \cdots, \hat{u}_{N-2}^{n+1})^T,\\
U^{n-1} &= (\hat{u}_0^{n-1}, \hat{u}_1^{n-1}, \hat{u}_2^{n-1}, \cdots, \hat{u}_{N-2}^{n-1})^T,\\
F^n &= (F_0^n, F_1^n, F_2^n, \cdots, F_{N-2}^n)^T,\\
F_i^n &= (f(\cdot, t_n), \phi_i(\cdot)).
\end{aligned}
$$

After solving the linear system (8), the numerical solution of $u(x,t)$ at (x_k, t_n) is

$$
u_N^n(x_k) = \sum_{j=0}^{N-2} \hat{u}_j^n (L_j(\hat{x}_k) - L_{j+2}(\hat{x}_k)), \quad k = 0, 1, \cdots, N. \tag{9}
$$

where $\hat{x}_k$, $k = 0, 1, \cdots, N$ are Legendre–Gauss quadrature nodes, i.e., zeros of $L_{N+1}(\hat{x})$ [45].

3.1. Stability and Convergence Analysis for Semi-Discrete and Fully Discrete Schemes

In this subsection, we perform a stability and convergence analysis of the semi-discrete scheme (4) and the fully discrete scheme (6). Let

$$
A(u,v) = K_1 c_{\alpha_1} A^{\alpha_1}(u,v) + K_2 c_{\alpha_2} A^{\alpha_2}(u,v),
$$

where

$$
A^{\alpha_k}(u,v) = \left({}_aD_x^{\alpha_k/2}u, {}_xD_b^{\alpha_k/2}v\right) + \left({}_xD_b^{\alpha_k/2}u, {}_aD_x^{\alpha_k/2}v\right), k = 1, 2.
$$

For simplicity, we use $\|\cdot\|$ to stand for $\|\cdot\|_{\mathcal{L}^2(\Omega)}$ afterwards. The seminorm $|\cdot|_{P,Q}$ and the norm $\|\cdot\|_{P,Q}$ are defined as

$$
|u|_{P,Q} = \left(K_1 \|{}_aD_x^{\alpha_1/2}u\|^2 + K_2\|{}_aD_x^{\alpha_2/2}u\|^2\right)^{1/2},
$$

$$
\|u\|_{P,Q} = (\|u\|^2 + |u|_{P,Q}^2)^{1/2}.
$$

Lemma 7 ([45])**.** *Let $s, r \in \mathbb{R}$, and $0 \le s \le r$. Then, there exists a constant C such that for any $u \in H_0^s \cap H_0^r$, the following inequality holds:*

$$
\|u - \Pi_N^{1,0}u\|_s \le CN^{s-r}\|u\|_r,
$$

where $\Pi_N^{1,0}$ is the orthogonal projection operator.

The orthogonal projection operator $\Pi_N^{P,Q} : H_0^{\alpha_1/2} \cap H_0^{\alpha_2/2} \to V_N$ is defined as

$$
A(u - \Pi_N^{P,Q}u, v) = 0, \quad \forall v \in V_N. \tag{10}
$$

Lemma 8. *Let $r \in \mathbb{R}$, $\Omega = (a,b)$. If α_1, α_2 satisfy $0 < \alpha_1/2, \alpha_2/2 < 1 < r$ and $\alpha_1 \ne 1/2$, then there exist constants C independent of N such that $\forall u \in H_0^{\alpha_1}(\Omega) \cap H_0^{\alpha_2}(\Omega) \cap H_0^r(\Omega)$, and the following inequality holds:*

$$
|u - \Pi_N^{P,Q}u|_{P,Q} \le CN^{\alpha_1/2-r}\|u\|_r + CN^{\alpha_2/2-r}\|u\|_r.
$$

Proof. From the definition of the seminorm $|\cdot|_{P,Q}$, combined with the properties of the orthogonal projection operator $\Pi_N^{P,Q}$, we have

$$\begin{aligned}|u-\Pi_N^{P,Q}u|_{P,Q}^2 &= A(u-\Pi_N^{P,Q}u, u-\Pi_N^{P,Q}u) = A(u-\Pi_N^{P,Q}u, u-u_N)\\ &\leq C|u-\Pi_N^{P,Q}u|_{P,Q}|u-u_N|_{P,Q}.\end{aligned}$$

Letting $u_N = \Pi_N^{1,0}u$ and using Lemma 7 leads to

$$\begin{aligned}|u-\Pi_N^{P,Q}u|_{P,Q} &\leq C|u-\Pi_N^{1,0}|_{P,Q}\\ &\leq C\Big(N^{\alpha_1/2-r}\|u\|_r + N^{\alpha_2/2-r}\|u\|_r\Big).\end{aligned}$$

□

To evaluate a numerical algorithm, we need to discuss its stability first. Generally speaking, a numerical method is stable if the numerical solution can be bounded from above by the data that are supplied to the problem with a constant that does not depend on the discretization parameters. In other words, the result does not "explode" numerically [47]. Next, we will present the theorem of the stability of the semi-discrete scheme (4).

Theorem 1 (Stability of semi-discrete scheme)**.** *Let u^{n+1} be the solution of problem* (2) *in the semi-discrete scheme* (4)*. Then, the semi-discrete scheme is stable, and there exists a positive constant C independent of n and τ such that*

$$\|u^{n+1}\|_{P,Q} \leq C\left(|u^0|_{P,Q}^2 + 2\tau\sum_{k=1}^{n}\|f^k\|^2\right)^{1/2}.$$

Proof. We have the following weak form of (4) for $v \in V_N$:

$$\Big(\delta_{\hat{t}}u^k, v\Big) = K_1\left(\frac{\partial^{\alpha_1}}{\partial|x|^{\alpha_1}}u^{\bar{k}}, v\right) + K_2\left(\frac{\partial^{\alpha_2}}{\partial|x|^{\alpha_2}}u^{\bar{k}}, v\right) + \Big(f^k, v\Big).$$

Substituting v by $\delta_{\hat{t}}u^k$, the above equation becomes

$$\|\delta_{\hat{t}}u^k\|^2 = K_1\left(\frac{\partial^{\alpha_1}}{\partial|x|^{\alpha_1}}u^{\bar{k}}, \delta_{\hat{t}}u^k\right) + K_2\left(\frac{\partial^{\alpha_2}}{\partial|x|^{\alpha_2}}u^{\bar{k}}, \delta_{\hat{t}}u^k\right) + \Big(f^k, \delta_{\hat{t}}u^k\Big).$$

After the application of the Cauchy–Schwarz inequality and the mean inequality chain, we have

$$\Big(f^k, \delta_{\hat{t}}u^k\Big) \leq \frac{1}{2}\Big(\|f^k\|^2 + \|\delta_{\hat{t}}u^k\|^2\Big) \leq \frac{1}{2}\|f^k\|^2 + \|\delta_{\hat{t}}u^k\|^2,$$

and hence,

$$0 \leq K_1\left(\frac{\partial^{\alpha_1}}{\partial|x|^{\alpha_1}}u^{\bar{k}}, \delta_{\hat{t}}u^k\right) + K_2\left(\frac{\partial^{\alpha_2}}{\partial|x|^{\alpha_2}}u^{\bar{k}}, \delta_{\hat{t}}u^k\right) + \frac{1}{2}\|f^k\|^2. \quad (11)$$

According to the definition of $A^{\alpha_k}(u,v)$, it holds that

$$\begin{aligned}K_1\left(\frac{\partial^{\alpha_1}}{\partial|x|^{\alpha_1}}u^{\bar{k}}, \delta_{\hat{t}}u^k\right) &= \frac{K_1c_{\alpha_1}}{4\tau}\Big(A^{\alpha_1}(u^{k+1},u^{k+1}) - A^{\alpha_1}(u^{k-1},u^{k-1})\Big)\\ &= \frac{K_1}{4\tau}\Big(\|{}_{-\infty}D_x^{\alpha_1/2}\hat{u}^{k-1}\|_{\mathcal{L}^2(\mathbb{R})}^2 - \|{}_{-\infty}D_x^{\alpha_1/2}\hat{u}^{k+1}\|_{\mathcal{L}^2(\mathbb{R})}^2\Big),\\ K_2\left(\frac{\partial^{\alpha_2}}{\partial|x|^{\alpha_2}}u^{\bar{k}}, \delta_{\hat{t}}u^k\right) &= \frac{K_2c_{\alpha_2}}{4\tau}\Big(A^{\alpha_2}(u^{k+1},u^{k+1}) - A^{\alpha_2}(u^{k-1},u^{k-1})\Big)\\ &= \frac{K_2}{4\tau}\Big(\|{}_{-\infty}D_x^{\alpha_2/2}\hat{u}^{k-1}\|_{\mathcal{L}^2(\mathbb{R})}^2 - \|{}_{-\infty}D_x^{\alpha_2/2}\hat{u}^{k+1}\|_{\mathcal{L}^2(\mathbb{R})}^2\Big),\end{aligned}$$

where $\hat{u}$ is the extension of u by zero outside Ω. Therefore,

$$\begin{aligned}
&K_1\left(\frac{\partial^{\alpha_1}}{\partial|x|^{\alpha_1}}u^{\bar{k}},\delta_{\hat{t}}u^k\right)+K_2\left(\frac{\partial^{\alpha_2}}{\partial|x|^{\alpha_2}}u^{\bar{k}},\delta_{\hat{t}}u^k\right)\\
&=\frac{1}{4\tau}\left(K_1\|{}_{-\infty}D_x^{\alpha_1/2}\hat{u}^{k-1}\|^2_{\mathcal{L}^2(\mathbb{R})}+K_2\|{}_{-\infty}D_x^{\alpha_2/2}\hat{u}^{k-1}\|^2_{\mathcal{L}^2(\mathbb{R})}\right)\\
&-\frac{1}{4\tau}\left(K_1\|{}_{-\infty}D_x^{\alpha_1/2}\hat{u}^{k+1}\|^2_{\mathcal{L}^2(\mathbb{R})}+K_2\|{}_{-\infty}D_x^{\alpha_2/2}\hat{u}^{k+1}\|^2_{\mathcal{L}^2(\mathbb{R})}\right)\\
&=\frac{1}{4\tau}\left(K_1\|{}_aD_x^{\alpha_1/2}u^{k-1}\|^2+K_2\|{}_aD_x^{\alpha_2/2}u^{k-1}\|^2\right)\\
&-\frac{1}{4\tau}\left(K_1\|{}_aD_x^{\alpha_1/2}u^{k+1}\|^2+K_2\|{}_aD_x^{\alpha_2/2}u^{k+1}\|^2\right)\\
&=\frac{1}{4\tau}\left(|u^{k-1}|^2_{P,Q}-|u^{k+1}|^2_{P,Q}\right).
\end{aligned}$$

Equation (11) hence can be reduced to

$$|u^{k+1}|^2_{P,Q}\le|u^{k-1}|^2_{P,Q}+2\tau\|f^k\|^2. \tag{12}$$

Letting k in (12) vary from 1 to n and adding the equations together yield

$$|u^n|^2_{P,Q}+|u^{n+1}|^2_{P,Q}\le|u^0|^2_{P,Q}+|u^1|^2_{P,Q}+2\tau\sum_{k=0}^{n}\|f^k\|^2.$$

From Lemma 6, there exists C such that $C\|u^{n+1}\|^2_{P,Q}\le|u^{n+1}|^2_{P,Q}$; thus,

$$\begin{aligned}
C\|u^{n+1}\|^2_{P,Q}\le|u^{n+1}|^2_{P,Q}&<|u^n|^2_{P,Q}+|u^{n+1}|^2_{P,Q}\\
&\le|u^0|^2_{P,Q}+|u^1|^2_{P,Q}+2\tau\sum_{k=0}^{n}\|f^k\|^2\\
&\le|u^0|^2_{P,Q}+\frac{1}{2}(|u^0|^2_{P,Q}+|u^2|^2_{P,Q})+2\tau\sum_{k=0}^{n}\|f^k\|^2\\
&=\frac{3}{2}|u^0|^2_{P,Q}+\frac{1}{2}|u^2|^2_{P,Q}+2\tau\sum_{k=0}^{n}\|f^k\|^2\\
&\le2|u^0|^2_{P,Q}+\tau\|f^1\|^2+2\tau\sum_{k=0}^{n}\|f^k\|^2\\
&\le2(|u^0|^2_{P,Q}+2\tau\sum_{k=0}^{n}\|f^k\|^2).
\end{aligned}$$

□

According to the above theorem, when the function $\int_\Omega f^2(x,t)dx\in\mathcal{L}^2(I)$, then $\tau\sum_{k=0}^{n}\|f^k\|^2$ is finite, and hence, the semi-discrete scheme (4) is stable. In the following, the convergence of the semi-discrete scheme (4) is presented.

Theorem 2 (Convergence of semi-discrete scheme)**.** *Assume that u is the exact solution of Equation (2), and u^n is the numerical solution of the semi-discrete scheme (4). Then, there exists a constant C independent of k and τ such that*

$$\|u^n(\cdot)-u(\cdot,t_n)\|_{P,Q}\le C\tau^2.$$

Proof. Subtracting (3) from (4) and taking the inner product with $v\in V_n$ on both sides, we have

$$\left(\delta_{\hat{t}}\theta^k,v\right)=K_1\left(\frac{\partial^{\alpha_1}}{\partial|x|^{\alpha_1}}\theta^{\bar{k}},v\right)+K_2\left(\frac{\partial^{\alpha_2}}{\partial|x|^{\alpha_2}}\theta^{\bar{k}},v\right)+\left(H_1^k,v\right), \tag{13}$$

where $\theta^k(x) = u^k(x) - u(x, t_k)$ and $H_1^k = O(\tau^2)$.

Taking $v = \delta_{\hat{t}}\theta^k$ and using a similar technique to that used for the proof of Theorem 1, we have

$$\|\theta^{n+1}\|_{P,Q} \leq C\left(|\theta^0|_{P,Q}^2 + 2\tau\sum_{k=1}^{n}\|H_1^k\|^2\right)^{1/2}.$$

As can be seen from the above, there exists a constant C such that

$$\|u^n(\cdot) - u(\cdot, t_n)\|_{P,Q} \leq C\tau^2. \tag{14}$$

□

By using a similar approach to that used for the proof of Theorem 1, we can obtain the stability result of the fully discrete scheme as in the below theorem.

Theorem 3 (Stability of the fully discrete scheme)**.** *Let u_N^{n+1} be the numerical solution of the fully discrete scheme* (6)*. Then, the scheme is stable, and there exists a positive constant C independent of N, n, and τ such that*

$$\|u_N^{n+1}\|_{P,Q} \leq C\left(|u_N^0|_{P,Q}^2 + 2\tau\sum_{k=1}^{n}\|f^k\|^2\right)^{1/2}.$$

Theorem 4 (Convergence of the fully discrete scheme)**.** *Assume that $u \in H^3((0,T]; H^r((a,b)))$ is the exact solution of Equation* (2)*, and u_N^n is the numerical solution obtained in scheme* (6)*. Then, there exists a positive constant C independent of n, N, and τ such that*

$$\|u_N^n(\cdot) - u(\cdot, t_n)\|_{P,Q} \leq C\left(\tau^2 + N^{\alpha_1/2-r} + N^{\alpha_2/2-r}\right).$$

Proof. Taking the inner product with $v \in V_n$ on both sides of (3) and then subtracting (6) from it, we have

$$\left(\delta_{\hat{t}}e^k, v\right) = K_1\left(\frac{\partial^{\alpha_1}}{\partial|x|^{\alpha_1}}e^{\bar{k}}, v\right) + K_2\left(\frac{\partial^{\alpha_2}}{\partial|x|^{\alpha_2}}e^{\bar{k}}, v\right) + \left(H_1^k, v\right), \tag{15}$$

where $e^k(x) = u(x, t_k) - u_N^k(x)$ and $H_1^k = O(\tau^2)$.

Let $\xi^k = u(x, t_k) - \Pi_N^{P,Q}u(x, t_k)$ be the projection error and $\eta^k = \Pi_N^{P,Q}u(x, t_k) - u_N^k(x)$ be the error between the projection of the exact solution and the numerical solution; hence,

$$e^k(x) = u(x, t_k) - \Pi_N^{P,Q}u(x, t_k) + \Pi_N^{P,Q}u(x, t_k) - u_N^k(x) := \xi^k(x) + \eta^k(x). \tag{16}$$

Next, we need to estimate $|\eta^k|_{P,Q}$. By the definition of the orthogonal projection operator $\Pi_N^{P,Q}$, Equation (15) can be rewritten as

$$\left(\delta_{\hat{t}}\eta^k, v\right) = K_1\left(\frac{\partial^{\alpha_1}}{\partial|x|^{\alpha_1}}\eta^{\bar{k}}, v\right) + K_2\left(\frac{\partial^{\alpha_2}}{\partial|x|^{\alpha_2}}\eta^{\bar{k}}, v\right) + \left(H_2^k, v\right), \tag{17}$$

where $H_2^k = -\delta_{\hat{t}}\xi^k + O(\tau^2)$.

Taking the test function $v = \delta_{\hat{t}}\eta^k$ and adding k from 1 to n in (17) yields

$$\|\eta^{n+1}\|_{P,Q} \leq C\left(|\eta^0|_{P,Q}^2 + 2\tau\sum_{k=1}^{n}\|H_2^k\|^2\right)^{1/2}.$$

To show the convergence of the fully discrete scheme (6), it is only necessary to estimate the upper bounds of $|\eta^0|_{P,Q}$ and $\|H_2^k\|$.

For $|\eta^0|_{P,Q}$, by Lemmas 7 and 8, we have

$$\begin{aligned}|\eta^0|_{P,Q} \leq \|\eta^0\|_{P,Q} &= \|\Pi_N^{P,Q} u_0 - \Pi_N^{1,0} u_0\|_{P,Q} \\ &\leq \|\Pi_N^{P,Q} u_0 - u_0\|_{P,Q} + \|u_0 - \Pi_N^{1,0} u_0\|_{P,Q} \\ &\leq C\Big(N^{\alpha_1/2-r} + N^{\alpha_2/2-r}\Big).\end{aligned}$$

Since $H_2^k = -\delta_{\hat{t}}\xi^k + O(\tau^2)$, we only need to estimate $\|\delta_{\hat{t}}\xi^k\|$. For $\|\delta_{\hat{t}}\xi^k\|$, we have

$$\|\delta_{\hat{t}}\xi^k\|_{P,Q} \leq C|\delta_{\hat{t}}\xi^k|_{P,Q} \leq C\Big(N^{\alpha_1/2-r} + N^{\alpha_2/2-r}\Big).$$

Above all, we have

$$\|u_N^k - u(x,t_k)\|_{P,Q} \leq C\Big(\tau^2 + N^{\alpha_1/2-r} + N^{\alpha_2/2-r}\Big).$$

□

3.2. Implementation of Fully Discrete Scheme

We will give the details of the computation of the matrices in the scheme (8).

Computation of the matrix M**.** The ith-row–jth-column of the matrix M is the inner product of ϕ_j and ϕ_i:

$$\begin{aligned}(M)_{i,j} = (\phi_j, \phi_i) &= \int_a^b \phi_j(x)\phi_i(x)dx \\ &= \int_a^b (L_j(\hat{x}) - L_{j+2}(\hat{x}))(L_i(\hat{x}) - L_{i+2}(\hat{x}))dx \\ &= \frac{b-a}{2}\int_{-1}^1 (L_j(\hat{x}) - L_{j+2}(\hat{x}))(L_i(\hat{x}) - L_{i+2}(\hat{x}))d\hat{x}.\end{aligned}$$

Due to the orthogonality of Legendre polynomials, we have

$$(M)_{ij} = \begin{cases} \frac{b-a}{2}\Big(\frac{2}{2i+1} + \frac{2}{2i+5}\Big), & i = j, \\ -\frac{b-a}{2i+1}, & i = j+2, \\ -\frac{b-a}{2i+5}, & i = j-2, \\ 0, & \text{else}. \end{cases} \tag{18}$$

Computation of the matrix S**.** The matrix S^α contains important components of S. It follows that

$$\begin{aligned}(S^\alpha)_{ij} &= \Big({}_aD_x^{\alpha/2}\phi_j, {}_xD_b^{\alpha/2}\phi_i\Big) \\ &= \Big({}_aD_x^{\alpha/2}L_j(\hat{x}), {}_xD_b^{\alpha/2}L_i(\hat{x})\Big) - \Big({}_aD_x^{\alpha/2}L_{j+2}(\hat{x}), {}_xD_b^{\alpha/2}L_i(\hat{x})\Big) \\ &- \Big({}_aD_x^{\alpha/2}L_j(\hat{x}), {}_xD_b^{\alpha/2}L_{i+2}\hat{x})\Big) + \Big({}_aD_x^{\alpha/2}L_{j+2}(\hat{x}), {}_xD_b^{\alpha/2}L_{i+2}(\hat{x})\Big) \\ &\triangleq T(j,i) - T(j+2,i) - T(j,i+2) + T(j+2,i+2).\end{aligned} \tag{19}$$

According to (19), we need to calculate $T(j,i) = \left({}_aD_x^{\alpha/2}L_j(\hat{x}), {}_xD_b^{\alpha/2}L_i(\hat{x})\right)$ to compute $(S^\alpha)_{ij}$. Applying Lemma 2 yields

$$\begin{aligned} T(j,i) &= \left({}_aD_x^{\alpha/2}L_j(\hat{x}), {}_xD_b^{\alpha/2}L_i(\hat{x})\right) \\ &= (\frac{b-a}{2})^{-\alpha}\left({}_{-1}D_{\hat{x}}^{\alpha/2}L_j(\hat{x}), {}_{\hat{x}}D_1^{\alpha/2}L_i(\hat{x})\right) \\ &= (\frac{b-a}{2})^{-\alpha}\int_a^b {}_{-1}D_{\hat{x}}^{\alpha/2}L_j(\hat{x})_{\hat{x}}D_1^{\alpha/2}L_i(\hat{x})dx \\ &= (\frac{b-a}{2})^{-\alpha}\mathcal{G}_{i,j}^\alpha\int_a^b(1+\hat{x})^{-\alpha/2}(1-\hat{x})^{-\alpha/2}J_j^{\alpha/2,-\alpha/2}(\hat{x})J_i^{-\alpha/2,\alpha/2}(\hat{x})dx \\ &= (\frac{b-a}{2})^{1-\alpha}\mathcal{G}_{i,j}^\alpha\int_{-1}^1(1+\hat{x})^{-\alpha/2}(1-\hat{x})^{-\alpha/2}J_j^{\alpha/2,-\alpha/2}(\hat{x})J_i^{-\alpha/2,\alpha/2}(\hat{x})d\hat{x} \\ &\approx (\frac{b-a}{2})^{1-\alpha}\mathcal{G}_{i,j}^\alpha\sum_{k=0}^N\omega_k^{-\alpha/2,-\alpha/2}J_j^{\alpha/2,-\alpha/2}(\hat{x}_k)J_i^{-\alpha/2,\alpha/2}(\hat{x}_k), \end{aligned} \tag{20}$$

where

$$\mathcal{G}_{i,j}^\alpha = \frac{\Gamma(j+1)\Gamma(i+1)}{\Gamma(j-\alpha/2+1)\Gamma(i-\alpha/2+1)}.$$

We have used the Jacobi–Gauss quadrature rule in the last step of (20), where $\hat{x}_k$ and $\omega_k^{-\alpha/2,-\alpha/2}$, $k = 0,1,\ldots,N$, are Jacobi–Gauss quadrature nodes and the corresponding weights [45].

Computation of the vector F^n. Noting that $F_i^n = (f^n, \phi_i)$, we have

$$\begin{aligned} F_i^n &= \int_a^b f(x,t_n)\phi_i(x)dx \\ &= \frac{b-a}{2}\int_{-1}^1 f(x,t_n)\phi_i(x)d\hat{x} \\ &= \frac{b-a}{2}\int_{-1}^1 f(x,t_n)(L_i(\hat{x})-L_{i+2}(\hat{x}))d\hat{x} \\ &\approx \frac{b-a}{2}\sum_{k=0}^N f(x_k,t_n)(L_i(\hat{x}_k)-L_{i+2}(\hat{x}_k))\omega_k, \quad i=0,\ldots N-2, \end{aligned} \tag{21}$$

where

$$x_k = \frac{b-a}{2}\hat{x}_k + \frac{b+a}{2} \in [a,b]. \tag{22}$$

We have used the Legendre–Gauss quadrature rule in the last step of (21), where $\hat{x}_k$ and $\omega_k, k = 0,1,\ldots,N$ are Legendre–Gauss quadrature nodes and the corresponding weights [45].

4. Spectral Galerkin Methods for Two-Dimensional Riesz Space-Fractional Convection–Diffusion Equation

In this section, as an extension of the previous section, we present the spectral Galerkin method for the two-dimensional Riesz space-fractional convection–diffusion equations.

Consider the following convection–diffusion equations for $0 < \alpha_1,\ \beta_1 < 1, 1 < \alpha_2,\ \beta_2 < 2$:

$$\begin{aligned} \frac{\partial u(x,y,t)}{\partial t} &= K_1\frac{\partial^{\alpha_1}u(x,y,t)}{\partial|x|^{\alpha_1}} + K_2\frac{\partial^{\beta_1}u(x,y,t)}{\partial|y|^{\beta_1}} \\ &\quad + K_3\frac{\partial^{\alpha_2}u(x,y,t)}{\partial|x|^{\alpha_2}} + K_4\frac{\partial^{\beta_2}u(x,y,t)}{\partial|y|^{\beta_2}} + f(x,y,t),\ (x,y,t)\in\Omega_2\times I \\ u(x,y,0) &= u_0(x,y), (x,y)\in\Omega_2, \\ u(x,y,t) &= 0, (x,y,t)\in\partial\Omega_2\times I, \end{aligned} \tag{23}$$

where $I = (0, T]$ is the time interval, $\Omega_2 = (a_1, b_1) \times (a_2, b_2)$ is the spatial domain, $u(x, y, t)$ denotes the solute concentration, K_1 and K_2 denote the fluid velocities in the x- and y-directions, respectively, K_3 and K_4 denote the diffusion coefficients, and $f(x, y, t)$ is the source function.

Let

$$\begin{aligned} F_x u(x,y,t) &= K_1 \frac{\partial^{\alpha_1} u(x,y,t)}{\partial |x|^{\alpha_1}} + K_3 \frac{\partial^{\alpha_2} u(x,y,t)}{\partial |x|^{\alpha_2}}, \\ F_y u(x,y,t) &= K_2 \frac{\partial^{\beta_1} u(x,y,t)}{\partial |y|^{\beta_1}} + K_4 \frac{\partial^{\beta_2} u(x,y,t)}{\partial |y|^{\beta_2}}. \end{aligned} \tag{24}$$

Then, Equation (23) can be written as

$$\frac{\partial u}{\partial t} = F_x u + F_y u + f(x,y,t). \tag{25}$$

We will give the fully discrete scheme for (25) in the next step.

In the time direction, applying the same technique to (25) yields

$$\delta_{\hat{t}} u^n = (F_x + F_y) u^{\bar{n}} + f^n. \tag{26}$$

By adding $\tau^2 F_x F_y \delta_{\hat{t}} u^n$ to the left-hand side of (26), we obtain

$$\delta_{\hat{t}} u^n + \tau^2 F_x F_y \delta_{\hat{t}} u^n = (F_x + F_y) u^{\bar{n}} + f^n + O(\tau^2).$$

The above equation can also be written as

$$(1 - \tau F_x)(1 - \tau F_y) u^{n+1} = (1 + \tau F_x)(1 + \tau F_y) u^{n-1} + 2\tau f^n + O(\tau^3). \tag{27}$$

Subsequently, several function spaces are introduced.

The function spaces V_N^x and V_N^y are defined as

$$\begin{aligned} V_N^x &= \operatorname{span}\{\phi_i(x) : i = 0, 1, \cdots, N-2\}, \\ V_N^y &= \operatorname{span}\{\varphi_j(y) : j = 0, 1, \cdots, N-2\}, \end{aligned}$$

where

$$\begin{aligned} \phi_i(x) &= L_i(\hat{x}) - L_{i+2}(\hat{x}), \quad \hat{x} \in [-1,1], \quad x = \frac{b-a}{2}\hat{x} + \frac{a+b}{2} \in [a,b], \\ \varphi_j(y) &= L_j(\hat{y}) - L_{j+2}(\hat{y}), \quad \hat{y} \in [-1,1], \quad y = \frac{d-c}{2}\hat{y} + \frac{c+d}{2} \in [c,d]. \end{aligned}$$

The function space S_N on Ω is thus given by

$$S_N = V_N^x \otimes V_N^y = \operatorname{span}\{\phi_i(x)\varphi_j(y), \quad i, j = 0, 1, \cdots, N-2\}. \tag{28}$$

The numerical solution of (25) is obtained by finding $u_N^n \in S_N$ such that, for any $v \in S_N$, the following is satisfied:

$$\begin{cases} \Big((1 - \tau F_x)(1 - \tau F_y) u_N^{n+1}, v\Big) = \Big((1 + \tau F_x)(1 + \tau F_y) u_N^{n-1}, v\Big) + 2\tau (f^n, v), \\ u_N^0 = \Pi_N^{1,0} u_0, \end{cases} \tag{29}$$

where $\Pi_N^{1,0}$ is the projection operator satisfying

$$\Big(\Pi_N^{1,0} u - u, v\Big) + \Big(\partial_x(\Pi_N^{1,0} u - u), \partial_x v\Big) + \Big(\partial_y(\Pi_N^{1,0} u - u), \partial_y v\Big) = 0, \quad \forall v \in S_N.$$

Equation (29) is the fully discrete scheme of problem (25).

Since $u_N^{n+1} \in S_N$, we have

$$u_N^{n+1} = \sum_{i=0}^{N-2} \sum_{j=0}^{N-2} \hat{u}_{i,j}^{n+1} \phi_i(x) \varphi_j(y). \tag{30}$$

Let $v = \phi_i \varphi_j$ $(i, j = 0, 1, \cdots, N-2)$, and we can obtain the matrix representation of (29) as follows:

$$(M_x - \tau S_x) U^{n+1} (M_y - \tau S_y)^T = (M_x + \tau S_x) U^{n-1} (M_y + \tau S_y)^T + 2\tau F^n, \tag{31}$$

where

$$\begin{aligned}
&(M_x)_{ij} = (\phi_j, \phi_i), \quad (M_y)_{ij} = (\varphi_j, \varphi_i), \\
&(S_x)_{ij} = K_1 c_{\alpha_1} (S_x^{\alpha_1} + (S_x^{\alpha_1})^T) + K_3 c_{\alpha_2} (S_x^{\alpha_2} + (S_x^{\alpha_2})^T), \\
&(S_y)_{ij} = K_2 c_{\beta_1} (S_y^{\beta_1} + (S_y^{\beta_1})^T) + K_4 c_{\beta_2} (S_y^{\beta_2} + (S_y^{\beta_2})^T), \\
&(S_x^{\alpha_k})_{ij} = \left({}_a D_x^{\alpha_k/2} \phi_j, {}_x D_b^{\alpha_k/2} \phi_i \right), \\
&(S_y^{\beta_k})_{ij} = \left({}_c D_y^{\beta_k/2} \varphi_j, {}_y D_d^{\beta_k/2} \varphi_i \right), \\
&(U^{n+1})_{ij} = \hat{u}_{ij}^{n+1}, \\
&(U^{n-1})_{ij} = \hat{u}_{ij}^{n-1}, \\
&(F^n)_{ij} = (f^n, \phi_i \varphi_j), \quad i, j = 0, 1, \cdots, N-2.
\end{aligned}$$

After solving the linear system (31), the numerical solution of $u(x, y, t)$ at (x_k, y_l, t_{n+1}) is given by

$$u_N^{n+1}(x_k, y_l) = \sum_{k=0}^{N-2} \sum_{l=0}^{N-2} \hat{u}_{ij}^{n+1} (L_i(\hat{x}_k) - L_{i+2}(\hat{x}_k))(L_j(\hat{y}_l) - L_{j+2}(\hat{y}_l)), \quad k, l = 0, 1, \cdots, N,$$

where $\hat{x}_k$ and $\hat{y}_l$ are the Legendre–Gauss quadrature nodes.

The computation formulas of M_x, M_y, $S_x^{\alpha_k}$, and $S_y^{\beta_k}$ are provided in (18)–(20) in Section 3, and $(F^n)_{ij}$ can be computed by using the two-dimensional Legendre–Gauss quadrature rule.

Stability and Convergence

In this subsection, we demonstrate the stability and convergence of the semi-discrete scheme (27) and the fully discrete scheme (29). Before presenting the theorem, we list a few necessary notations and lemmas first.

Let

$$A(u, v) = K_1 c_{\alpha_1} A_x^{\alpha_1}(u, v) + K_2 c_{\beta_1} A_y^{\beta_1}(u, v) + K_3 c_{\alpha_2} A_x^{\alpha_2}(u, v) + K_4 c_{\beta_2} A_x^{\beta_2}(u, v),$$

where

$$\begin{aligned}
A_x^{\alpha_k} &= \left({}_a D_x^{\alpha_k/2} u, {}_x D_b^{\alpha_k/2} v \right) + \left({}_x D_b^{\alpha_k/2} u, {}_a D_x^{\alpha_k/2} v \right), \\
A_y^{\beta_k} &= \left({}_c D_y^{\beta_k/2} u, {}_y D_d^{\beta_k/2} v \right) + \left({}_y D_d^{\beta_k/2} u, {}_c D_y^{\beta_k/2} v \right).
\end{aligned}$$

Define the orthogonal projection operator $\Pi_N^{P,Q} : H_0^{\alpha/2} \cap H_0^{\beta/2} \rightarrow S_N$, satisfying

$$A(u - \Pi_N^{P,Q} u, v) = 0, \quad \forall v \in S_N,$$

where $\alpha = \max\{\alpha_1, \alpha_2\}$, $\beta = \max\{\beta_1, \beta_2\}$.

The seminorm $|\cdot|_{P,Q}$ and the norm $\|\cdot\|_{P,Q}$ are defined as

$$\begin{aligned}|u|_{P,Q} &= (K_1\|_aD_x^{\alpha_1/2}u\|^2 + K_2\|_cD_y^{\beta_1/2}u\|^2 \\ &\quad + K_3\|_aD_x^{\alpha_2/2}u\|^2 + K_4\|_cD_y^{\beta_2/2}u^2_{\mathcal{L}^2(\mathbb{R}^2)})^{1/2}, \\ \|u\|_{P,Q} &= \left(\|u\|^2 + |u|^2_{P,Q}\right)^{1/2}.\end{aligned}$$

Lemma 9. *Let $r \in \mathbb{R}$. If $0 < \alpha_k/2, \beta_k/2 < 1 < r$ and $\alpha_k/2,\ \beta_k/2 \neq 1/2$, then there exists a constant C independent of N such that for any $u \in H_0^{\alpha/2}(\Omega) \cap H_0^{\beta/2}(\Omega) \cap H^r(\Omega)$, the following inequality holds:*

$$|u - \Pi_N^{P,Q}u|_{P,Q} \leq C\left(N^{\alpha_1/2-r}\|u\|_r + N^{\alpha_2/2-r}\|u\|_r + N^{\beta_1/2-r}\|u\|_r + N^{\beta_2/2-r}\|u\|_r\right).$$

Proof. The proof is similar to that of Lemma 8. □

Theorem 5 (Stability of the semi-discrete scheme)**.** *Let u^{n+1} be the solution of the two-dimensional problem (25) in the semi-discrete scheme (27). Then, the semi-discrete scheme (27) is stable, and there exists a positive constant C independent of n and τ such that*

$$\|u^{n+1}\|_{P,Q} \leq C\left(|u^0|^2_{P,Q} + 2\tau\sum_{k=1}^{n}\|f^k\|^2\right)^{1/2}.$$

Theorem 6 (Convergence of the semi-discrete scheme)**.** *Assume that u is the exact solution of Equation (23), and u^n is the solution of the semi-discrete scheme (27). Then, there exists a constant C independent of k and τ such that*

$$\|u^n - u(x,y,t_n)\|_{P,Q} \leq C\tau^2.$$

Theorem 7. *(Stability of the fully discrete scheme). Assume that u_N^{n+1} is the solution of the fully discrete scheme (29), then the scheme is stable, and there exists a positive constant C independent of N, n, and τ such that*

$$\|u_N^{n+1}\|_{P,Q} \leq C\left(|u_N^0|^2_{P,Q} + 2\tau\sum_{k=1}^{n}\|f^k\|^2\right)^{1/2}.$$

Theorem 8 (Convergence of the fully discrete scheme)**.** *Assume that $u \in H^3(I; H^r(\Omega))$ is the exact solution of Equation (23), and u_N^k is the numerical solution obtained in the scheme (29). Then, there exists a positive constant C independent of n, N, and τ such that*

$$\|u_N^n - u(x,y,t_n)\|_{P,Q} \leq C\left(\tau^2 + N^{\alpha_1/2-r} + N^{\alpha_2/2-r} + N^{\beta_1/2-r} + N^{\beta_2/2-r}\right).$$

The approach to performing error analysis for two-dimensional problems is consistent with the one-dimensional case. However, it is worth noting that in two-dimensional problems, we need to prove $\left(F_xF_y\delta_{\hat{t}}u^k, \delta_{\hat{t}}u^k\right) \geq 0$. In the following, we will provide the details of the proof.

By definition, for $\forall v \in S_N$, we have

$$\begin{aligned}(F_xF_yv, v) &= K_1K_2\left(\frac{\partial^{\alpha_1}}{\partial|x|^{\alpha_1}}\frac{\partial^{\beta_1}}{\partial|y|^{\beta_1}}v, v\right) + K_1K_4\left(\frac{\partial^{\alpha_1}}{\partial|x|^{\alpha_1}}\frac{\partial^{\beta_2}}{\partial|y|^{\beta_2}}v, v\right) \\ &\quad + K_3K_2\left(\frac{\partial^{\alpha_2}}{\partial|x|^{\alpha_2}}\frac{\partial^{\beta_1}}{\partial|y|^{\beta_1}}v, v\right) + K_3K_4\left(\frac{\partial^{\alpha_2}}{\partial|x|^{\alpha_2}}\frac{\partial^{\beta_2}}{\partial|y|^{\beta_2}}v, v\right),\end{aligned} \tag{32}$$

where

$$\left(\frac{\partial^{\alpha_1}}{\partial|x|^{\alpha_1}}\frac{\partial^{\beta_1}}{\partial|y|^{\beta_1}}v, v\right) = 2c_{\alpha_1}c_{\beta_1}\left({}_aD_x^{\alpha_1/2}{}_cD_y^{\beta_1/2}v, {}_xD_b^{\alpha_1/2}{}_yD_d^{\beta_1/2}v\right) + 2c_{\alpha_1}c_{\beta_1}\left({}_aD_x^{\alpha_1/2}{}_yD_d^{\beta_1/2}v, {}_xD_b^{\alpha_1/2}{}_cD_y^{\beta_1/2}v\right).$$

Define a bilinear form as

$$A^{(\alpha,\beta)}(u,v) = \left({}_aD_x^{\alpha/2}{}_yD_d^{\beta/2}u, {}_xD_b^{\alpha/2}{}_cD_y^{\beta/2}v\right) + \left({}_aD_x^{\alpha/2}{}_cD_y^{\beta/2}u, {}_xD_b^{\alpha/2}{}_yD_d^{\beta/2}v\right).$$

Equation (32) hence becomes

$$\left(F_xF_yv, v\right) = 2K_1K_2c_{\alpha_1}c_{\beta_1}A^{(\alpha_1,\beta_1)}(v,v) + 2K_1K_4c_{\alpha_1}c_{\beta_2}A^{(\alpha_1,\beta_2)}(v,v) + 2K_3K_2c_{\alpha_2}c_{\beta_1}A^{(\alpha_2,\beta_1)}(v,v) + 2K_3K_4c_{\alpha_2}c_{\beta_2}A^{(\alpha_2,\beta_2)}(v,v).$$

According to Lemma 5, we have

$$\begin{aligned} 2c_\alpha c_\beta A^{(\alpha,\beta)} &= 2c_\alpha c_\beta\left(\left({}_aD_x^{\alpha/2}{}_yD_d^{\beta/2}v, {}_xD_b^{\alpha/2}{}_cD_y^{\beta/2}v\right) + \left({}_aD_x^{\alpha/2}{}_cD_y^{\beta/2}v, {}_xD_b^{\alpha/2}{}_yD_d^{\beta/2}v\right)\right) \\ &= 4c_\alpha c_\beta\cos(\alpha\pi/2)\cos(\beta\pi/2)\|{}_{-\infty}D_x^{\alpha/2}{}_{-\infty}D_y^{\beta/2}\hat{v}\|^2_{\mathcal{L}^2(\mathbb{R}^2)} \\ &= \|{}_{-\infty}D_x^{\alpha/2}{}_{-\infty}D_y^{\beta/2}\hat{v}\|^2_{\mathcal{L}^2(\mathbb{R}^2)}, \end{aligned}$$

and then,

$$\begin{aligned} \left(F_xF_yv, v\right) &= K_1K_2\|{}_{-\infty}D_x^{\alpha_1/2}{}_{-\infty}D_y^{\beta_1/2}\hat{v}\|^2_{\mathcal{L}^2(\mathbb{R}^2)} + K_1K_4\|{}_{-\infty}D_x^{\alpha_1/2}{}_{-\infty}D_y^{\beta_2/2}\hat{v}\|^2_{\mathcal{L}^2(\mathbb{R}^2)} \\ &+ K_3K_2\|{}_{-\infty}D_x^{\alpha_2/2}{}_{-\infty}D_y^{\beta_1/2}\hat{v}\|^2_{\mathcal{L}^2(\mathbb{R}^2)} + K_3K_4\|{}_{-\infty}D_x^{\alpha_2/2}{}_{-\infty}D_y^{\beta_2/2}\hat{v}\|^2_{\mathcal{L}^2(\mathbb{R}^2)}, \end{aligned}$$

where $\hat{v}$ is the extension of v by zero outside Ω_2. Obviously, we have

$$\left(F_xF_y\delta_{\hat{t}}u^k, \delta_{\hat{t}}u^k\right) \geq 0.$$

5. Numerical Results

In this section, some numerical examples are presented to illustrate the theoretical analysis.

The MATLAB (R2023a) platform was used for all numerical simulations in this paper. Equations (8) and (31) were solved directly by using "/" and "\" in MATLAB.

To begin with, we define $\mathcal{L}^\infty$ and $\mathcal{L}^2$ errors for $d = 1$ and $d = 2$, respectively. For $d = 1$, define

$$\begin{aligned} \mathrm{err}_{\mathcal{L}^\infty}|_{t=t_n} &:= \max_{0\leq k\leq N}|u(x_k,t_n) - u_N^n(x_k)|, \\ \mathrm{err}_{\mathcal{L}^2}|_{t=t_n} &:= \left(\frac{b-a}{2}\sum_{0\leq k\leq N}\omega_k|u(x_k,t_n) - u_N^n(x_k)|^2\right)^{1/2}; \end{aligned}$$

for $d = 2$, define

$$\begin{aligned} \mathrm{err}_{\mathcal{L}^\infty}|_{t=t_n} &:= \max_{0\leq k,l\leq N}|u(x_k,y_j,t_n) - u_N^n(x_k,y_l)|, \\ \mathrm{err}_{\mathcal{L}^2}|_{t=t_n} &:= \left(\frac{(b_1-a_1)(b_2-a_2)}{4}\sum_{0\leq k\leq N}\sum_{0\leq l\leq N}\omega_k\omega_l|u(x_k,y_l,t_n) - u_N^n(x_k,y_l)|^2\right)^{1/2}, \end{aligned}$$

where x_k, y_l are defined as in (22), and ω_k, ω_l are the corresponding weights in the Legendre–Gauss quadrature rule.

Subsequently, we will provide four examples and plot the results of numerical simulations by using a sufficiently small time step for these examples.

Example 1. *We consider the Riesz space-fractional convection–diffusion equation as in* (2)*:*
The source function of the problem is

$$f(x,t) = f_0(x,t) + f_1(x,t) + f_2(x,t),$$

where

$$f_0(x,t) = t^{\mu-1}(\mu+\nu t)e^{\nu t}x^2(1-x)^2,$$

$$\begin{aligned} f_1(x,t) = &-K_1 c_{\alpha_1} t^{\mu} e^{\nu t}\Big(\frac{2}{\Gamma(3-\alpha_1)}(x^{2-\alpha_1}+(1-x)^{2-\alpha_1}) \\ &- \frac{12}{\Gamma(4-\alpha_1)}(x^{3-\alpha_1}+(1-x)^{3-\alpha_1}) + \frac{24}{\Gamma(5-\alpha_1)}(x^{4-\alpha_1}+(1-x)^{4-\alpha_1})\Big), \\ f_2(x,t) = &-K_2 c_{\alpha_2} t^{\mu} e^{\nu t}\Big(\frac{2}{\Gamma(3-\alpha_2)}(x^{2-\alpha_2}+(1-x)^{2-\alpha_2}) \\ &- \frac{12}{\Gamma(4-\alpha_2)}(x^{3-\alpha_2}+(1-x)^{3-\alpha_2}) + \frac{24}{\Gamma(5-\alpha_2)}(x^{4-\alpha_2}+(1-x)^{4-\alpha_2})\Big). \end{aligned}$$

The exact solution of the problem is

$$u(x,t) = t^{\mu}e^{\nu t}x^2(1-x)^2, \quad x \in [0,L],\ t \in [0,T].$$

Example 1 can also be found in [37].

Example 2. *In this example, we consider the Riesz space-fractional convection–diffusion equation as in* (2)*. The source function is*

$$f(x,t) = f_0(x,t) + f_1(x,t) + f_2(x,t),$$

where

$$\begin{aligned} f_0(x,t) &= (1-t)e^{-t}\sin(\pi x), \\ f_1(x,t) &= -K_1 c_{\alpha_1} t e^{-t}(h_{l1}(x) + h_{r1}(x)), \\ f_2(x,t) &= -K_2 c_{\alpha_2} t e^{-t}(h_{l2}(x) + h_{r2}(x)). \end{aligned}$$

The formulas for h_{l1}, h_{r1}, h_{l2}, and h_{r2} are as follows:

$$\begin{aligned} h_{l1}(x) &= {}_0D_x^{\alpha_1}\sin(\pi x) \\ &= \frac{\pi(2-\alpha_1)x^{1-\alpha_1}F_2(1;\frac{3}{2}-\frac{\alpha_1}{2},2-\frac{\alpha_1}{2};-\frac{1}{4}\pi^2x^2)}{\Gamma(1-\alpha_1)(\alpha_1^2-3\alpha_1+2)} \\ &- \frac{\pi^3x^{3-\alpha_1}F_2(2;\frac{5}{2}-\frac{\alpha_1}{2},3-\frac{\alpha_1}{2};-\frac{1}{4}\pi^2x^2)}{2\Gamma(1-\alpha_1)(\frac{3}{2}-\frac{\alpha_1}{2})(2-\frac{\alpha_1}{2})(\alpha_1^2-3\alpha_1+2)}, \end{aligned} \tag{33}$$

$$\begin{aligned} h_{r1}(x) &= {}_xD_L^{\alpha_1}\sin(\pi x) \\ &= \frac{(L-x)^{-\alpha_1}}{(\alpha_1-2)(\alpha_1-1)\Gamma(1-\alpha_1)}((\alpha_1-1)((\alpha_1-2)\sin(\pi L) \\ &- \pi^2(L-x)^2\sin(\pi x)F_2(1-\frac{\alpha_1}{2};\frac{3}{2},2-\frac{\alpha_1}{2};-\frac{1}{4}\pi^2(L-x)^2)) \\ &+ \pi(\alpha_1-2)(L-x)\cos(\pi x)F_2(\frac{1}{2}-\frac{\alpha_1}{2};\frac{1}{2},\frac{3}{2}-\frac{\alpha_1}{2};-\frac{1}{4}\pi^2(L-x)^2)), \end{aligned} \tag{34}$$

$$
\begin{aligned}
h_{l2}(x) &= {}_0D_x^{\alpha_2}\sin(\pi x) \\
&= \frac{\pi x^{1-\alpha_2}}{(\alpha_2-7)(\alpha_2-6)(\alpha_2-5)(\alpha_2-4)(\alpha_2^2-5\alpha_2+6)\Gamma(2-\alpha_2)} \\
&(2\pi^2x^2((2\alpha_2^3-33\alpha_2^2+175\alpha_2-294)F_2(2;3-\frac{\alpha_2}{2},\frac{7}{2}-\frac{\alpha_2}{2};-\frac{1}{4}\pi^2x^2) \\
&+4\pi^2x^2F_2(3;4-\frac{\alpha_2}{2},\frac{9}{2}-\frac{\alpha_2}{2};-\frac{1}{4}\pi^2x^2)) \\
&+(\alpha_2^6-27\alpha_2^5+295\alpha_2^4-1665\alpha_2^3)F_2(1;2-\frac{\alpha_2}{2},\frac{5}{2}-\frac{\alpha_2}{2};-\frac{1}{4}\pi^2x^2) \\
&+(5104\alpha_2^2-8028\alpha_2+5040)F_2(1;2-\frac{\alpha_2}{2},\frac{5}{2}-\frac{\alpha_2}{2};-\frac{1}{4}\pi^2x^2)),
\end{aligned}
\tag{35}
$$

$$
\begin{aligned}
h_{r2}(x) &= {}_xD_L^{\alpha_2}\sin(\pi x) \\
&= \frac{(L-x)^{-\alpha_2}}{(\alpha_2-3)(\alpha_2-2)\Gamma(2-\alpha_2)} \\
&(\pi^3(\alpha_2-2)(L-x)^3\cos(\pi x)F_2(\frac{3}{2}-\frac{\alpha_2}{2};\frac{3}{2},\frac{5}{2}-\frac{\alpha_2}{2};-\frac{1}{4}\pi^2(L-x)^2) \\
&+(\alpha_2-3)(\pi^2(L-x)^2\sin(\pi x)F_2(1-\frac{\alpha_2}{2};\frac{1}{2},2-\frac{\alpha_2}{2};-\frac{1}{4}\pi^2(L-x)^2) \\
&-(\alpha_2-2)((\alpha_2-1)\sin\pi L+\pi(L-x)\cos\pi L))),
\end{aligned}
\tag{36}
$$

where $F_2(\cdot;\cdot,\cdot;\cdot)$ is the hypergeometric function.

The exact solution of the problem is

$$u(x,t) = te^{-t}\sin(\pi x), \quad x\in[0,L],\ t\in[0,T].$$

Example 3. *We consider the Riesz space-fractional convection–diffusion equation in (23).*

The source function of the problem is chosen to be

$$f(x,y) = f_0(x,y) + te^{-t}(f_1(x,y)+f_2(x,y)+f_3(x,y)+f_4(x,y)),$$

where

$$f_0(x,y) = (1-t)e^{-t}x^2(1-x)^2y^2(1-y)^2,$$

and the formulas of f_1, f_2, f_3, and f_4 are listed as follows:

$$
\begin{aligned}
f_1(x,y) &= -K_1c_{\alpha_1}y^2(1-y)^2(\frac{2}{\Gamma(3-\alpha_1)}(x^{2-\alpha_1}+(1-x)^{2-\alpha_1}) \\
&-\frac{12}{\Gamma(4-\alpha_1)}(x^{3-\alpha_1}+(1-x)^{3-\alpha_1})+\frac{24}{\Gamma(5-\alpha_1)}(x^{4-\alpha_1}+(1-x)^{4-\alpha_1})),
\end{aligned}
\tag{37}
$$

$$
\begin{aligned}
f_2(x,y) &= -K_2c_{\beta_1}x^2(1-x)^2(\frac{2}{\Gamma(3-\beta_1)}(y^{2-\beta_1}+(1-y)^{2-\beta_1}) \\
&-\frac{12}{\Gamma(4-\beta_1)}(y^{3-\beta_1}+(1-y)^{3-\beta_1})+\frac{24}{\Gamma(5-\beta_1)}(y^{4-\beta_1}+(1-y)^{4-\beta_1})),
\end{aligned}
\tag{38}
$$

$$
\begin{aligned}
f_3(x,y) &= -K_3c_{\alpha_2}y^2(1-y)^2(\frac{2}{\Gamma(3-\alpha_2)}(x^{2-\alpha_2}+(1-x)^{2-\alpha_2}) \\
&-\frac{12}{\Gamma(4-\alpha_2)}(x^{3-\alpha_2}+(1-x)^{3-\alpha_2})+\frac{24}{\Gamma(5-\alpha_2)}(x^{4-\alpha_2}+(1-x)^{4-\alpha_2})),
\end{aligned}
\tag{39}
$$

$$f_4(x,y) = -K_4 c_{\beta_2} x^2(1-x)^2 \Big(\frac{2}{\Gamma(3-\beta_2)} (y^{2-\beta_2} + (1-y)^{2-\beta_2}) - \frac{12}{\Gamma(4-\beta_2)} (y^{3-\beta_2} + (1-y)^{3-\beta_2}) + \frac{24}{\Gamma(5-\beta_2)} (y^{4-\beta_2} + (1-y)^{4-\beta_2}) \Big). \tag{40}$$

The exact solution of the problem is

$$u(x,y,t) = te^{-t} x^2(1-x)^2 y^2 (1-y)^2, \quad (x,y) \in [0,L] \times [0,L],\ t \in [0,T]. \tag{41}$$

Example 4. *We consider the Riesz space-fractional convection–diffusion equation* (23).

The source function of the problem is

$$\begin{aligned} f(x,y,t) = &f_0(x,y,t) \\ &+ te^{-t} \sin(\pi y)[-K_1 c_{\alpha_1}(h_{l1}(x) + h_{r1}(x)) - K_3 c_{\alpha_2}(h_{l2}(x) + h_{r2}(x))] \\ &+ te^{-t} \sin(\pi x)[-K_2 c_{\beta_1}(h_{l1}(y) + h_{r1}(y)) - K_4 c_{\beta_2}(h_{l2}(y) + h_{r2}(y))], \end{aligned}$$

where

$$f_0(x,y,t) = (1-t)e^{-t} \sin(\pi x) \sin(\pi y).$$

The formulas for h_{l1}, h_{r1}, h_{l2}, and h_{r2} are provided in Equations (33)–(36).

The exact solution of the problem is

$$u(x,y) = te^{-t} \sin(\pi x) \sin(\pi y), \quad (x,y) \in [0,L] \times [0,L],\ t \in [0,T].$$

The time step is chosen to be $\tau = 10^{-4}$ to reduce the impact of the error in the time direction in the above numerical simulations. The numerical results for the fixed time step are plotted in Figures 1–8. The $\mathcal{L}^\infty$ and $\mathcal{L}^2$ errors between the exact solution and the numerical solution at $T = 1$ are plotted in log–log scale for Examples 1–4 in Figure 1, Figure 3, Figure 5, and Figure 7, respectively. We have sketched a reference line in the figures to show the approximate convergence rate. According to these error plots, it is easy to observe that as the number of nodes increases, the errors decrease rapidly, which is consistent with the conclusion of our error analysis. We picture the absolute values of the error point by point for both time and space intervals for Examples 1 and 2 at $N = 16$ in Figure 2 and Figure 4, respectively. For the two-dimensional problems, we have drawn the point-wise error plot at $T = 1$ by taking $N = 16$ and $N = 128$ for Example 3 in Figure 6 and taking $N = 16$ and $N = 256$ for Example 4 in Figure 8. It can be observed that the point-wise error estimates at the boundary are slightly higher, which is attributed to the singular kernel of the fractional-order differential operator.

In the following, we will provide the results of numerical comparison experiments for Example 1 with the finite difference method proposed in [37]. For this analysis, the time step in the simulations is chosen to be $1/N$. The experimental results are listed in Tables 1 and 2. From the data in the tables, one can see that our proposed method has higher accuracy and generally results in higher convergence orders. This is due to the spectral methods used in the spatial domain, which has spectral accuracy for smooth functions. The reason that the convergence order is much lower than that shown in Figure 1 is that our method results in a convergence rate of $O(\tau^2)$ in the time domain, which holds the total convergence rate back.

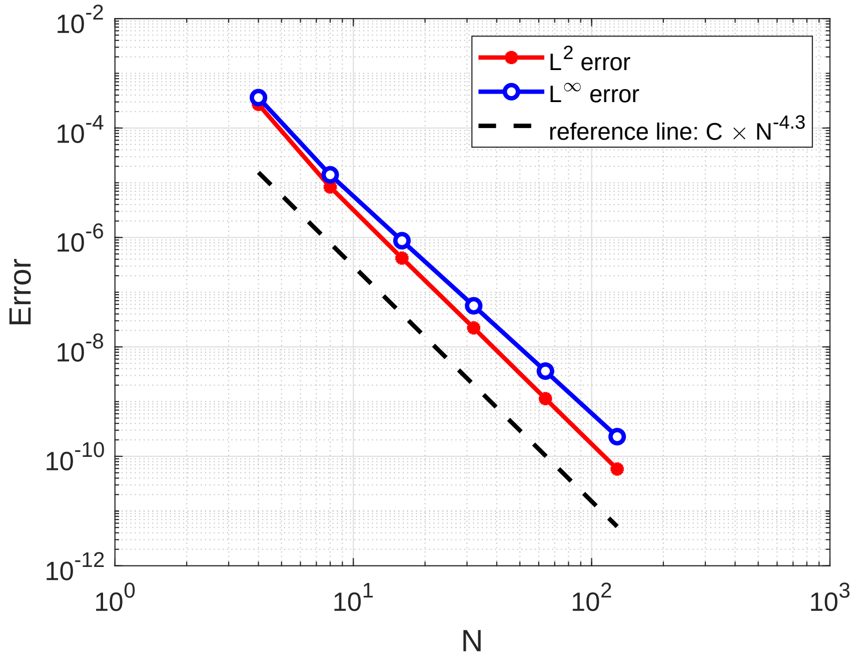

Figure 1. The $\mathcal{L}^\infty$ and $\mathcal{L}^2$ errors at $T = 1$ for Example 1 when $K_1 = K_2 = 1$, $L = 1$, $(\alpha_1, \alpha_2) = (0.6, 1.8)$, $\mu = 1$, $\nu = -1$, $\tau = 0.0001$, and $N = [4, 8, 16, 32, 46, 128]$.

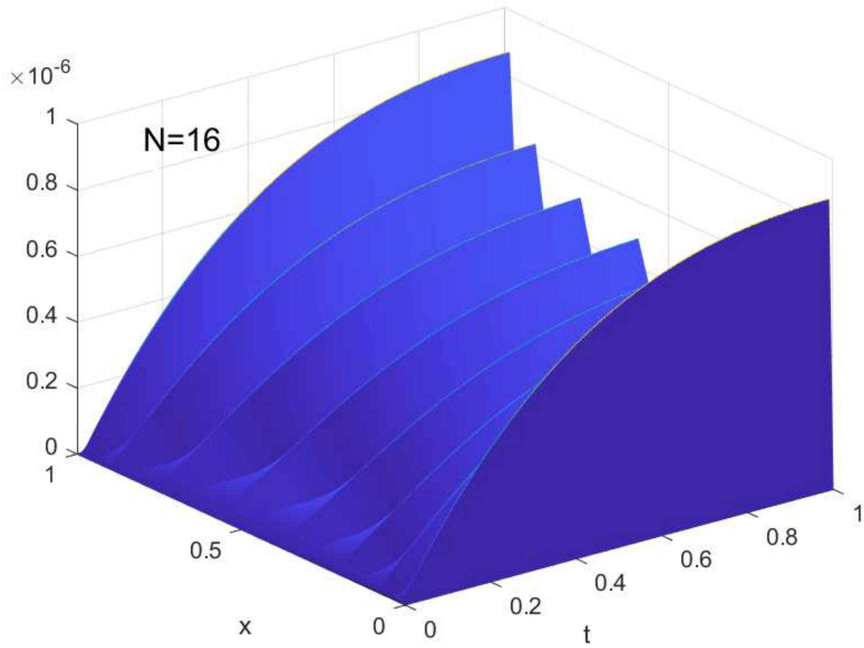

Figure 2. The point-wise error for Example 1 when $K_1 = K_2 = 1$, $L = 1$, $(\alpha_1, \alpha_2) = (0.6, 1.8)$, $\mu = 1$, $\nu = -1$, $\tau = 0.0001$, and $N = 16$.

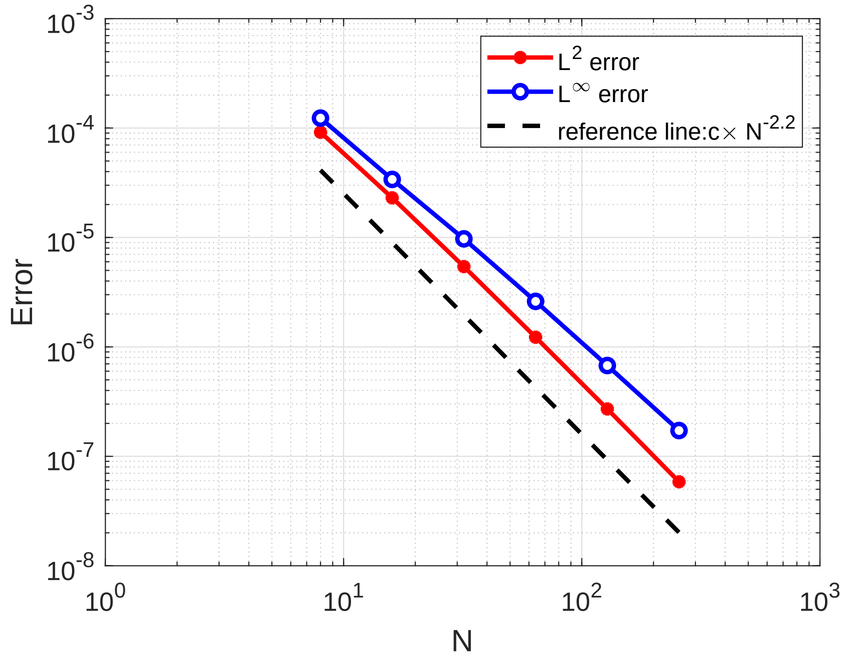

Figure 3. The $\mathcal{L}^\infty$ and $\mathcal{L}^2$ errors at $T = 1$ for Example 2 when $K_1 = K_2 = 1$, $L = 1$, $(\alpha_1, \alpha_2) = (0.6, 1.8)$, $\tau = 0.0001$, and $N = [8, 16, 32, 46, 128, 256]$.

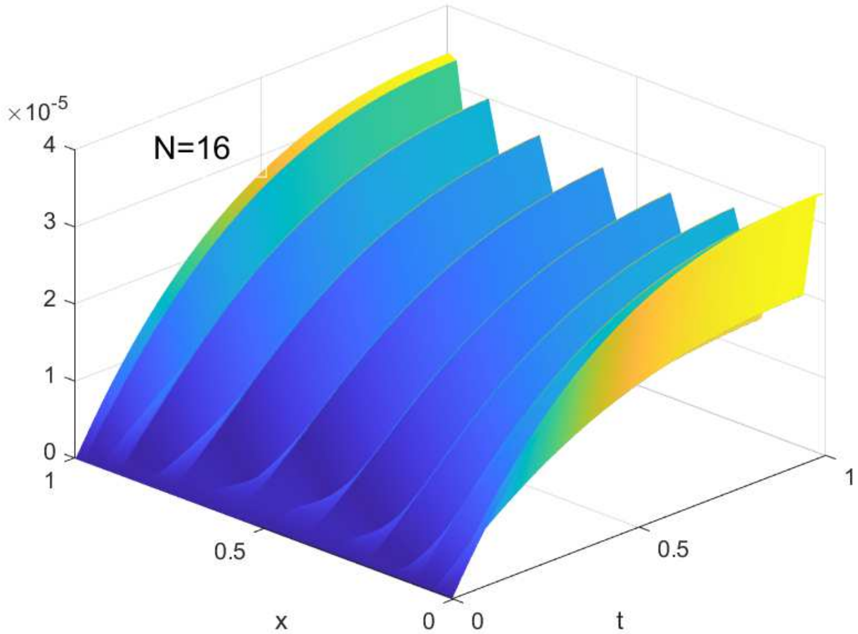

Figure 4. The point-wise error for Example 2 when $K_1 = K_2 = 1$, $L = 1$, $(\alpha_1, \alpha_2) = (0.6, 1.8)$, $\tau = 0.0001$, and $N = 16$.

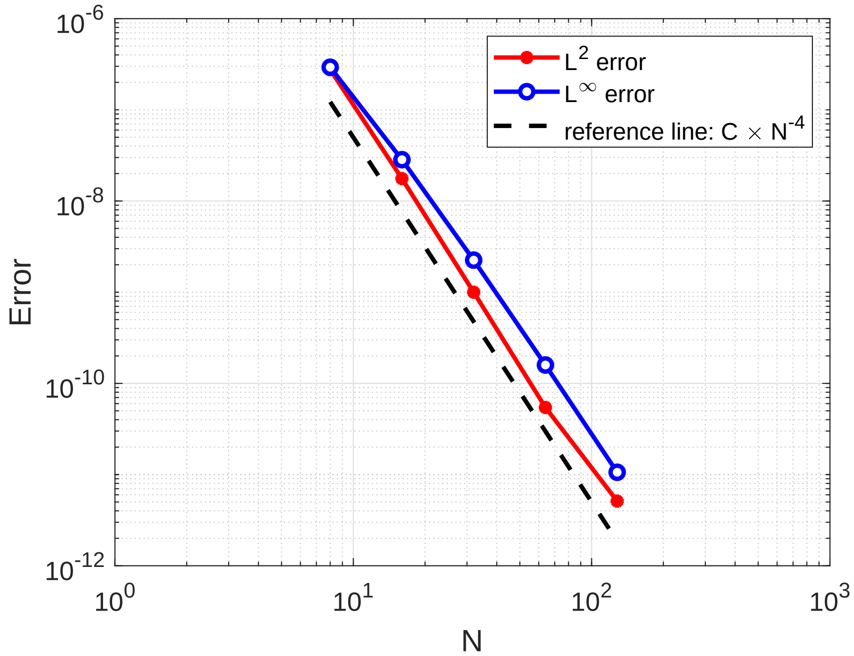

Figure 5. The $\mathcal{L}^\infty$ and $\mathcal{L}^2$ errors at $T = 1$ for Example 3 when $K_1 = K_2 = K_3 = K_4 = 1$, $L = 1$, $(\alpha_1, \alpha_2) = (0.6, 1.6)$, $(\beta_1, \beta_2) = (0.6, 1.8)$, $\tau = 0.0001$, and $N = [8, 16, 32, 46, 128]$.

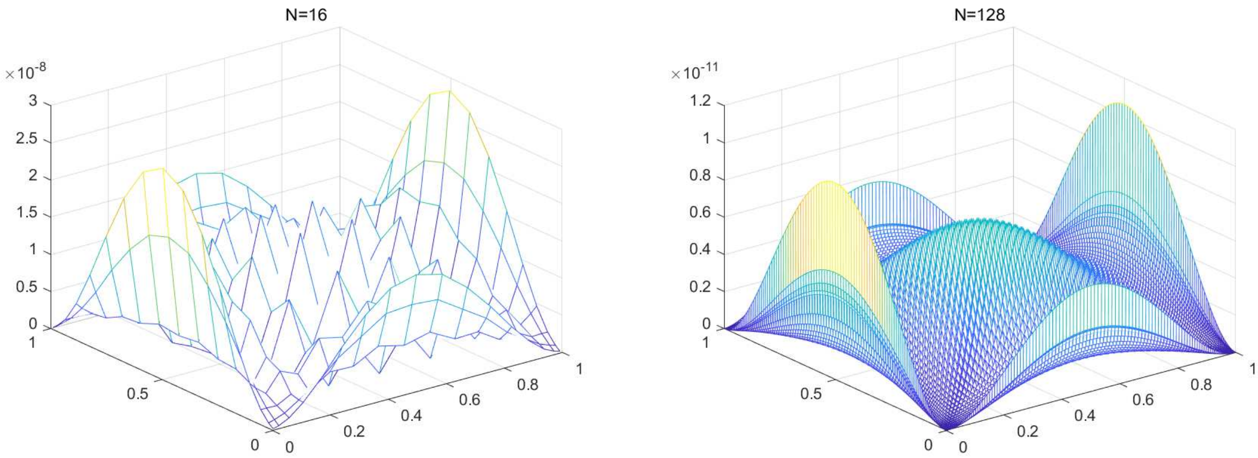

Figure 6. The point-wise error at $T = 1$ for Example 3 when $K_1 = K_2 = K_3 = K_4 = 1$, $L = 1$, $(\alpha_1, \alpha_2) = (0.6, 1.6)$, $(\beta_1, \beta_2) = (0.6, 1.8)$, and $\tau = 0.0001$. (**Left**): $N = 16$; (**Right**): $N = 128$.

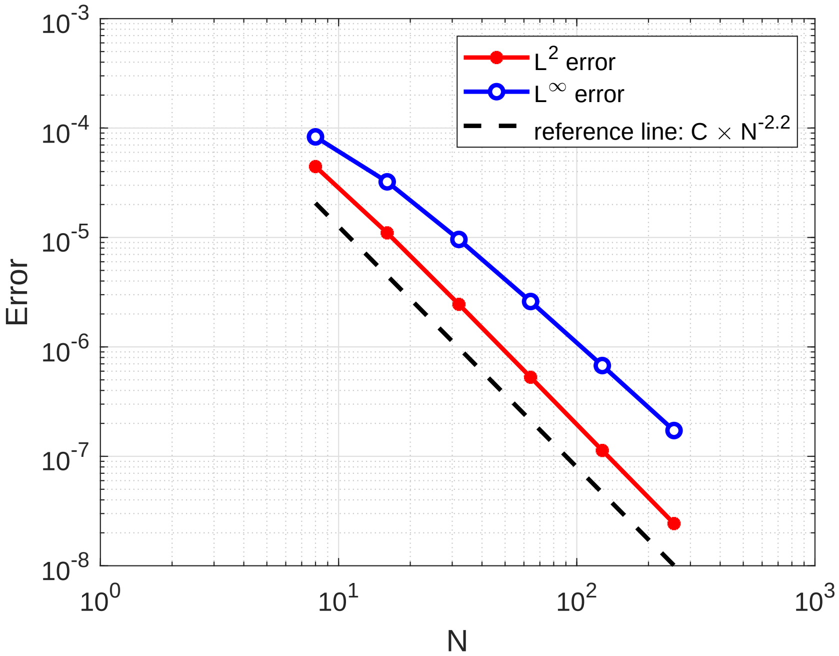

Figure 7. The $\mathcal{L}^\infty$ and $\mathcal{L}^2$ errors at $T = 1$ for Example 4 when $K_1 = K_2 = K_3 = K_4 = 1$, $L = 1$, $(\alpha_1, \alpha_2) = (0.2, 1.8)$, $(\beta_1, \beta_2) = (0.6, 1.8)$, $\tau = 0.0001$, and $N = [8, 16, 32, 46, 128, 256]$.

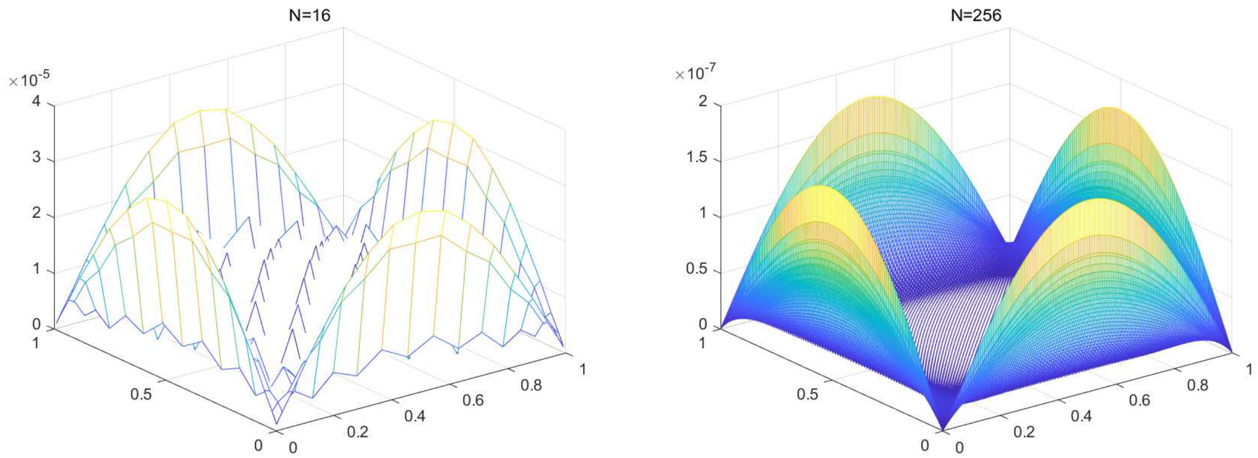

Figure 8. The point-wise error at $T = 1$ for Example 4 when $K_1 = K_2 = K_3 = K_4$, $L = 1$, $(\alpha_1, \alpha_2) = (0.2, 1.8)$, $(\beta_1, \beta_2) = (0.6, 1.8)$, and $\tau = 0.0001$. (**Left**): $N = 16$; (**Right**): $N = 256$.

Table 1. Convergence order and maximum error for Example 1, which is convection-dominant at $T = 1$ when $\nu = \alpha_1$, $\mu = \alpha_2$, $K_1 = 2$, and $K_2 = 0.25$.

		$\alpha_1 = 0.1$		$\alpha_1 = 0.45$		$\alpha_1 = 0.85$	
	$N(1/\tau)$	$\mathrm{err}_{\mathcal{L}^\infty}\|_{t=1}$	**Order**	$\mathrm{err}_{\mathcal{L}^\infty}\|_{t=1}$	**Order**	$\mathrm{err}_{\mathcal{L}^\infty}\|_{t=1}$	**Order**
	10	1.7575×10^{-4}	–	7.6952×10^{-4}	–	2.3088×10^{-3}	–
	20	3.3515×10^{-5}	2.3906	1.7774×10^{-4}	2.1142	5.3559×10^{-4}	2.1080
$\alpha_2 = 1.25$	40	5.1936×10^{-6}	2.6900	4.2000×10^{-5}	2.0813	1.2951×10^{-4}	2.0481
	80	1.0632×10^{-6}	2.2883	9.6456×10^{-6}	2.1224	3.1667×10^{-5}	2.0320
	160	6.5589×10^{-7}	0.6969	2.0735×10^{-6}	2.2178	7.7614×10^{-6}	2.0286

Table 1. *Cont.*

	$N(1/\tau)$	$\alpha_1 = 0.1$ $\text{err}_{\mathcal{L}^\infty}\|_{t=1}$	Order	$\alpha_1 = 0.45$ $\text{err}_{\mathcal{L}^\infty}\|_{t=1}$	Order	$\alpha_1 = 0.85$ $\text{err}_{\mathcal{L}^\infty}\|_{t=1}$	Order
$\alpha_2 = 1.85$	10	6.6256×10^{-4}	–	1.6599×10^{-3}	–	4.0506×10^{-3}	–
	20	1.6206×10^{-4}	2.0316	3.9472×10^{-4}	2.0722	9.3815×10^{-4}	2.1103
	40	4.0207×10^{-5}	2.0110	9.6426×10^{-5}	2.0333	2.2591×10^{-4}	2.0541
	80	9.9963×10^{-6}	2.0080	2.3816×10^{-5}	2.0175	5.5400×10^{-5}	2.0278
	160	2.4873×10^{-6}	2.0068	5.9151×10^{-6}	2.0094	1.3715×10^{-5}	2.0141

Table 2. Convergence order and maximum error for Example 1, which is diffusion-dominant at $T = 1$ when $\nu = \alpha_1$, $\mu = \alpha_2$, $K_1 = 0.25$, and $K_2 = 2$.

	$N(1/\tau)$	$\alpha_1 = 0.1$ $\text{err}_{\mathcal{L}^\infty}\|_{t=1}$	Order	$\alpha_1 = 0.45$ $\text{err}_{\mathcal{L}^\infty}\|_{t=1}$	Order	$\alpha_1 = 0.85$ $\text{err}_{\mathcal{L}^\infty}\|_{t=1}$	Order
$\alpha_2 = 1.25$	10	2.1908×10^{-4}	–	8.4270×10^{-4}	–	2.4135×10^{-3}	–
	20	4.9719×10^{-5}	2.1396	1.9674×10^{-4}	2.0987	5.5850×10^{-4}	2.1115
	40	1.2464×10^{-5}	1.9960	4.8421×10^{-5}	2.0226	1.3554×10^{-4}	2.0428
	80	3.0933×10^{-6}	2.0106	1.1983×10^{-5}	2.0146	3.3352×10^{-5}	2.0229
	160	7.6035×10^{-7}	2.0244	2.9711×10^{-6}	2.0119	8.2632×10^{-6}	2.0130
$\alpha_2 = 1.85$	10	7.2807×10^{-4}	–	1.8363×10^{-3}	–	4.4266×10^{-3}	–
	20	1.6902×10^{-4}	2.1069	4.2649×10^{-4}	2.1063	1.0152×10^{-3}	2.1244
	40	4.2081×10^{-5}	2.0059	1.0427×10^{-4}	2.0322	2.4453×10^{-4}	2.0537
	80	1.0500×10^{-5}	2.0028	2.5777×10^{-5}	2.0162	5.9981×10^{-5}	2.0274
	160	2.6225×10^{-6}	2.0014	6.4080×10^{-6}	2.0081	1.4852×10^{-5}	2.0139

6. Conclusions

In this paper, we studied spectral Galerkin methods for the one-dimensional and two-dimensional Riesz space-fractional convection–diffusion equations in (1).

Firstly, we developed the semi-discrete and fully discrete schemes of the one-dimensional equation in (2) using the CNLF scheme for discretization in the temporal direction and the spectral Galerkin–Legendre method for discretization in the spatial direction. We then rewrote the fully discrete form into a matrix-vector form, as in (8), and provided detailed calculation formulas for all matrices. Subsequently, we meticulously proved the theorems of stability and convergence for the semi-discrete and fully discrete schemes and showed that the schemes are stable with a convergence order of $O(\tau^2 + N^{\alpha_1/2-r} + N^{\alpha_2/2-r})$, where τ is the time step, $N+1$ is the number of spatial nodes, α_1 and α_2 are the orders of fractional derivatives, and r represents the smoothness of the function.

Secondly, we established the fully discrete format for two-dimensional problems, as in (23), in a similar way. We added a supplementary term $\tau^2 F_x F_y \delta_{\hat{t}} u^n$ to the left side of Equation (26), resulting in a symmetric fully discrete scheme. Next, we transformed the fully discrete form into a matrix-vector form, as in (31). Stability and convergence analyses of the semi-discrete and fully discrete schemes for two-dimensional problems were then presented, and the conclusions obtained were consistent with the one-dimensional case.

Finally, several numerical examples were designed, and the simulation results verified our theoretical study and analysis of our proposed numerical methods.

From the analysis and numerical results, we can see that the convergence rate in the temporal direction hinders the fast convergence rate in the spatial direction. In the future, we will study algorithms that apply spectral methods to both the time and space domains.

Author Contributions: Methodology, X.Z. (Xiaoyan Zeng); software, X.Z. (Xinxia Zhang), X.Z. (Xiaoyan Zeng); validation, J.W., Z.W. and Z.T.; writing—original draft preparation, X.Z. (Xinxia Zhang), X.Z. (Xiaoyan Zeng); writing—review and editing, J.W., Z.W. and Z.T. All authors have read and agreed to the published version of the manuscript.

Funding: This research was funded by the National Natural Science Foundation of China, grant number 11701358, 11774218

Data Availability Statement: No new data were created or analyzed in this study. Data sharing is not applicable to this article.

Conflicts of Interest: The authors declare no conflicts of interest.

References

1. Saichev, A.I.; Zaslavsky, G.M. Fractional Kinetic Equations: Solutions and Applications. *Chaos Interdiscip. J. Nonlinear Sci.* **1997**, *7*, 753–764. [CrossRef] [PubMed]
2. Mandelbrot, B.B.; Mandelbrot, B.B. *The Fractal Geometry of Nature*; WH Freeman: New York, NY, USA, 1982; pp. 54–96.
3. Mainardi, F. Some Basic Problem in Continum and Statistical Mechanics. *Fractals Fract. Calc. Contin. Mech.* **1997**, *378*, 291–348.
4. Bagley, R.L.; Torvik, P.J. A Theoretical Basis for the Application of Fractional Calculus to Viscoelasticity. *J. Rheol.* **1983**, *27*, 201–210. [CrossRef]
5. Bagley, R.L.; Torvik, P.J. Fractional Calculus in the Transient Analysis of Viscoelastically Damped Structures. *AIAA J.* **1985**, *23*, 918–925. [CrossRef]
6. Hilfer, R. *Applications of Fractional Calculus in Physics*; World Scientific: Singapore, 2000; pp. 10–25.
7. Scalas, E.; Gorenflo, R.; Mainardi, F. Fractional Calculus and Continuous-Time Finance. *Phys. A Stat. Mech. Its Appl.* **2000**, *284*, 376–384. [CrossRef]
8. Mainardi, F.; Raberto, M.; Gorenflo, R.; Scalas, E. Fractional Calculus and Continuous-Time Finance II: The Waiting-Time Distribution. *Phys. A Stat. Mech. Its Appl.* **2000**, *287*, 468–481. [CrossRef]
9. Wang, S.; Xu, M. Generalized Fractional Schrödinger Equation with Space-Time Fractional Derivatives. *J. Math. Phys.* **2007**, *48*, 2–10. [CrossRef]
10. Huang, F.; Liu, F. The Fundamental Solution of the Space-Time Fractional Advection-Dispersion Equation. *J. Appl. Math. Comput.* **2005**, *18*, 339–350.
11. El-Sayed, A.; Behiry, S.; Raslan, W. Adomian's Decomposition Method for Solving an Intermediate Fractional Advection-Dispersion Equation. *Comput. Math. Appl.* **2010**, *59*, 1759–1765. [CrossRef]
12. Golbabai, A.; Sayevand, K. Analytical Modelling of Fractional Advection-Dispersion Equation Defined in a Bounded Space Domain. *Math. Comput. Model.* **2010**, *53*, 1708–1718. [CrossRef]
13. Canuto, C.; Hussaini, M.Y.; Quarteroni, A.; Zang, T.A. *Spectral Methods: Fundamentals in Single Domains*; Springer Science & Business Media: Berlin/Heidelberg, Germany, 2007; pp. 20–35.
14. Santos, M.A.F. Analytic approaches of the anomalous diffusion: A review. *Chaos Solitons Fractals* **2019**, *124*, 86–96. [CrossRef]
15. Benson, D.A.; Wheatcraft, S.W. Meerschaert, M.M. Application of a Fractional Advection-Dispersion Equation. *Water Resour. Res.* **2000**, *36*, 1403–1412. [CrossRef]
16. Benson, D.A.; Wheatcraft, S.W.; Meerschaert, M.M. The Fractional-Order Governing Equation of Lévy Motion. *Water Resour. Res.* **2000**, *36*, 1413–1423. [CrossRef]
17. Metzler, R.; Klafter, J. The Random Walk's Guide to Anomalous Diffusion: A Fractional Dynamics Approach. *Phys. Rep.* **2000**, *339*, 1–77. [CrossRef]
18. Metzler, R.; Klafter, J. The Restaurant at the end of the Random Walk: Recent Developments in the Description of Anomalous Transport by Fractional Dynamics. *J. Phys. A Math. Gen.* **2004**, *37*, R161. [CrossRef]
19. Zaslavsky, G.M. Chaos, Fractional Kinetics and Anomalous transport. *Phys. Rep.* **2002**, *371*, 461–580. [CrossRef]
20. Schumer, R.; Benson, D.A. Meerschaert, M.M. Wheatcraft, S.W. Eulerian Derivation of the Fractional Advection-Dispersion Equation. *J. Contam. Hydrol.* **2001**, *48*, 69–88. [CrossRef]
21. Sun, Z.; Wu, X. A Fully Discrete Difference Scheme for a Diffusion-Wave System. *Appl. Numer. Math.* **2006**, *56*, 193–209. [CrossRef]
22. Liu, Q.; Liu, F.; Turner, I.; Anh, V. Approximation of the Lévy-Feller Advection-Dispersion Process by Random Walk and Finite Difference Method. *J. Comput. Phys.* **2007**, *222*, 57–70. [CrossRef]
23. Shen, S.; Liu, F.; Anh, V. Numerical Approximations and Solution Techniques for the Space-Time Riesz-Caputo Fractional Advection-Diffusion Equation. *Numer. Algorithms* **2011**, *56*, 383–403. [CrossRef]
24. Zhou, H.; Tian, W.; Deng, W. Quasi-Compact Finite Difference Schemes for Space Fractional Diffusion Equations. *J. Sci. Comput.* **2013**, *56*, 45–66. [CrossRef]
25. Wang, K.; Wang, H. A Fast Characteristic Finite Difference Method for Fractional Advection-Diffusion Equations. *Adv. Water Resour.* **2011**, *34*, 810–816. [CrossRef]
26. Huang, Q.; Huang, G.; Zhan, H. A Finite Element Solution for the Fractional Advection-Dispersion Equation. *Adv. Water Resour.* **2008**, *31*, 1578–1589. [CrossRef]
27. Lai, J.;Liu, F.; Anh, V.V.; Liu, Q. A space-time finite element method for solving linear Riesz space fractional partial differential equations. *Numer. Algorithms* **2021**, *88*, 499–520. [CrossRef]
28. Tang, H.; Xia, J. High-Order Accurate Runge-Kutta (Local) Discontinuous Galerkin Methods for One- and Two-Dimensional Fractional Diffusion Equations. *Numer. Math. Theory Methods Appl.* **2012**, *5*, 333–358. [CrossRef]

29. Bhrawy, A.H. A Jacobi Spectral Collocation Method for Solving Multi-Dimensional Nonlinear Fractional Sub-Diffusion Equations. *Numer. Algorithms* **2016**, *73*, 91–113. [CrossRef]
30. Bhrawy, A.H.; Zaky, M.A.; Van Gorder, R.A. A Space-Time Legendre Spectral Tau Method for the Two-Sided Space-Time Caputo Fractional Diffusion-Wave Equation. *Numer. Algorithms* **2016**, *71*, 151–180. [CrossRef]
31. Saadatmandi, A.; Dehghan, M.; Azizi, M.R. The Sinc-Legendre Collocation Method for a class of Fractional Convection-Diffusion Equations with Variable Coefficients. *Commun. Nonlinear Sci. Numer. Simul.* **2012**, *17*, 4125–4136. [CrossRef]
32. Shen, S.; Liu, F.; Anh, V.; Turner, I. The Fundamental Solution and Numerical Solution of the Riesz Fractional Advection-Dispersion Equation. *IMA J. Appl. Math.* **2008**, *73*, 850–872. [CrossRef]
33. Yang, Q.; Liu, F.; Turner, I. Numerical Methods for Fractional Partial Differential Equations with Riesz Space Fractional Derivatives. *Appl. Math. Model.* **2010**, *34*, 200–218. [CrossRef]
34. Zhang, H.; Liu, F.; Anh, V. Galerkin Finite Element Approximation of Symmetric Space-Fractional Partial Differential Equations. *Appl. Math. Comput.* **2010**, *217*, 2534–2545. [CrossRef]
35. Celik, C.; Duman, M. Crank-Nicolson Method for the Fractional Diffusion Equation with the Riesz Fractional Derivative. *J. Comput. Phys.* **2012**, *231*, 1743–1750. [CrossRef]
36. Zeng, F.; Liu, F.; Li, C.; Burrage, K.; Turner, I.; Anh, V. A Crank-Nicolson ADI Spectral Method for a Two-Dimensional Riesz Space Fractional Nonlinear Reaction-Diffusion Equation. *SIAM J. Numer. Anal.* **2014**, *52*, 2599–2622. [CrossRef]
37. Anley, E.F.; Zheng, Z. Finite Difference Method for Two-Sided Two Dimensional Space Fractional Convection-Diffusion Problem with Source Term. *Mathematics* **2020**, *8*, 1878. [CrossRef]
38. Basha, M.; Anley, E.F.; Dai, B. Linearized Crank–Nicolson Scheme for the Two-Dimensional Nonlinear Riesz Space-Fractional Convection–Diffusion Equation. *Fractal Fract.* **2023**, *7*, 240. [CrossRef]
39. Li, J.; Liu, F.; Feng, L.; Turner, I. A Novel Finite Volume Method for the Riesz Space Distributed-Order Diffusion Equation. *Comput. Math. Appl.* **2017**, *74*, 772–783. [CrossRef]
40. Li, J.; Liu, F.; Feng, L.; Turner, I. A Novel Finite Volume Method for the Riesz Space Distributed-Order Advection-Diffusion Equation. *Appl. Math. Model.* **2017**, *46*, 536–553. [CrossRef]
41. Ye, H.; Liu, F.; Anh, V.; Turner, I. Numerical Analysis for the Time Distributed-Order and Riesz Space Fractional Diffusions on Bounded Domains. *IMA J. Appl. Math.* **2015**, *80*, 825–838. [CrossRef]
42. Zhang, H.; Liu, F.; Jiang, X.; Zeng, F.; Turner, I. A Crank-Nicolson ADI Galerkin-Legendre Spectral Method for the Two-Dimensional Riesz Space Distributed-Order Advection-Diffusion Equation. *Comput. Math. Appl.* **2018**, *76*, 2460–2476. [CrossRef]
43. Hu, X,; Liu, F.; Turner, I.; Anh, V. An Implicit Numerical Method of a New Time Distributed-Order and Two-Sided Space-Fractional Advection-Dispersion Equation. *Numer. Algorithms* **2016**, *72*, 393–407. [CrossRef]
44. Ding, H.; Zhang, Y. New numerical methods for the Riesz space fractional partial differential equations, *Comput. Math. Appl.* **2012**, *63*, 1135–1146.
45. Shen, J.; Tang, T.; Wang, L. *Spectral Methods: Algorithms, Analysis and Applications*; Springer Science & Business Media: Berlin/Heidelberg, Germany, 2011.
46. Ervin, V.J.; Roop, J.P. Variational solution of fractional advection dispersion equations on bounded domains in R^d. *Numer. Methods Partial. Differ. Equ. Int. J.* **2007**, *23*, 256–281. [CrossRef]
47. Bærentzen, J.A.; Gravesen, J.; Anton, F.; Aanæs, H. Finite Difference Methods for Partial Differential Equations. In *Guide to Computational Geometry Processing*; Springer: London, UK, 2012; pp. 65–79.